

Diamond Exploration and Regional Prospectivity of Greenland

Mark T. Hutchison^{1,2}

✉ Mark T. Hutchison
mth@trigon-gs.com

¹ Department of Geology, Ministry for Business, Trade, Raw Materials, Justice and Equality, Government of Greenland, Imaneq 4, 3900 Nuuk, Greenland

² Trigon GeoServices Ltd., 2780 S. Jones Blvd, #35-15, Las Vegas, NV 89146, U.S.A.

Abstract

Greenland is dominated by cratonic nuclei that provide conditions for diamond formation. Pre-1.6 Ga rocks are exposed over 43% of ice-free land and many basins in younger areas evidence underlying Archean basement. Studies of mantle xenoliths reveal thick mantle lithosphere up to 220 km. Kimberlites, ultramafic lamprophyres, lamproites and carbonatites are exposed abundantly in almost all regions, and span 1632 Ma of geological time. A total of 3029 discrete diamond-prospective bedrock occurrences are known, mostly occurring as sheets but with diatremes and evidence for volcanoclastic rocks in the south. Known diamondiferous bodies are well represented over 930 km of Greenland's west coast. Recovered multi-carat diamonds and favourable mineral chemical data demonstrate the potential for diamondiferous bodies with large, good quality diamonds in potentially economic concentrations. Areas where pipes and diatremes are rare evidence extensive glacial erosion but retain the potential for better-preserved bodies to be discovered at high elevation and diamonds to be present offshore. Records of 120 334 good quality mineral chemical

27 analyses, allow a regional diamond prospectivity analysis of Greenland to be conducted.
28 Garnet, ilmenite, spinel, Cr-diopside and orthopyroxene all reveal mineral chemistries
29 consistent with diamond-stable mantle sources. All geographic subdivisions overlap
30 chemistries of indicators from diamond-producing areas of Canada. Quantitative prospectivity
31 modelling incorporating geophysical data shows that further opportunities exist for diamond
32 exploration in Greenland particularly in the North Atlantic and Rae Cratons of western
33 Greenland, the Ketilidian Orogen of southern Greenland, as well as within less-explored areas
34 such as the east and north, and off-shore.

35

36 **Keywords** Diamond • Greenland • kimberlite • mineral exploration • indicator minerals •
37 North Atlantic Craton • Rae Craton

38

39

40 **Introduction**

41

42 Greenland is dominated by cratonic nuclei to the Laurentia Super-craton (Pearson et al., 2021;
43 Figure 1), accreted episodically (Gardiner et al., 2020), and which provide conditions for the
44 formation of diamonds. Pre-1.6 Ga rocks are exposed over 43% of ice-free land and many
45 basins in younger areas evidence underlying Archean basement. Re-Os dating studies of the
46 mantle of west Greenland (Wittig et al., 2010) in particular, show consistent Archean and
47 Proterozoic ages. Therefore, younger rocks at the surface may in some cases act as cover over
48 diamondiferous rocks, rather than informing on the age and diamond prospectivity of the
49 underlying mantle. Studies of mantle xenoliths reveal thick mantle lithosphere to 220 km in
50 the North Atlantic Craton of western Greenland (Sand et al., 2009). Kimberlites, ultramafic
51 lamprophyres (UML) and lamproites are known to be exposed in almost all regions, and span
52 1632 Ma of geological time (Larsen and Rex, 1992; Secher et al., 2009; Hutchison et al.,

53 2024). Including also carbonatites, 3029 discrete bedrock diamond-prospective occurrences
54 have been identified (Figure 1), mostly occurring as dykes and sills. Known diamondiferous
55 bodies are well represented over 930 km of Greenland's west coast, most notably the Garnet
56 Lake four metre-thick composite aillikite / kimberlite sheet at Sarfartoq (Hutchison and Frei,
57 2009), and metamorphosed ultramafic lamprophyre sheets at Qeqertaa, Disko Bay (Bernstein
58 et al., 2013). Data from these, and other localities, demonstrate that Greenland is a host for
59 diamondiferous bodies with large, good quality diamonds in potentially economic
60 concentrations, with potential for future discovery.

61 Fifty years of diamond research and exploration have generated abundant data,
62 particularly from western and southern Greenland (Jensen et al., 2004; Hutchison, 2020a).
63 While climate and remoteness provide challenges to exploration and mineral development, it
64 is clear from the abundance of diamondiferous bodies and extent of prior exploration, that
65 considerable scope exists for future diamond exploration in Greenland. This study aims to
66 provide a framework for such exploration by reviewing the methods and efficacy of past
67 work, applying modern methods of data interpretation to the internally consistent and large
68 database of mineral chemical data of Hutchison (2020a), and applying established regional
69 prospectivity modelling methods to Greenland data.

70

71

72 **Methodology**

73

74 Records of 24 996 Greenland exploration samples allow an assessment of the methodologies
75 of past exploration and, combined with 120 334 good quality mineral chemical analyses
76 (Hutchison, 2020a), allow regional diamond prospectivity modelling of Greenland to be
77 conducted. In this study, critique of exploration methodologies predominantly relies upon
78 industry reports submitted to government (with references compiled in Hutchison, 2020a and

79 2022), and prospectivity modelling follows a two-part approach. A quantitative modelling
80 approach is framed by mantle lithosphere thickness, the age of surface rocks in the context of
81 being cover over potential diamond deposits, and the density of sampling combined with
82 recovery of visually-determined indicators. A mineral approach inspects diamond
83 concentrations and physical features, and compares and contrasts indicator mineral chemistry
84 among Greenlandic geological regions and with the diamond fields of neighbouring Canada.
85 The approach to prospectivity analysis broadly follows the strategies and techniques
86 developed for the Northern Territory of Australia and Western Australia (Hutchison, 2013 and
87 Hutchison, 2018a), with modifications described herein.

88

89 **Regional subdivisions**

90

91 In order to rank different parts of Greenland in terms of diamond prospectivity, a geographical
92 subdivision must be employed. The subdivision needs to create a number of discrete
93 geographical regions that are numerous enough to constrain the explorer to reasonably small
94 areas, but not so large a list as to assign few data to individual subdivisions and thus
95 becoming statistically questionable. The geographical areas should be based also on distinct
96 geological settings and identified age ranges which are as small as practical.

97 The solid geology of Greenland has been divided into onshore geological regions at 1:2 500
98 000 scale by Escher and Pulvertaft (1995). Because these regions are defined on the basis of
99 surface and near-surface solid geology, they do not necessarily identify regions affected by
100 the mantle conditions that control the likelihood of diamond formation. However, they do
101 divide Greenland into areas of different geological ages that are relevant to the likelihood of
102 near surface diamond occurrence, should underlying mantle conditions be favourable. Taking
103 into account the area of ice-free land, the Escher and Pulvertaft (1995) subdivisions compare
104 well in number to the subdivisions used in prior prospectivity analyses in Australia

105 (Hutchison, 2012 and 2018b). Therefore, the Escher and Pulvertaft (1995) subdivisions have
106 been employed with modifications where the North Atlantic Craton (NAC) and Rae Craton
107 have been subdivided, with the NAC split between east and western Greenland and the Rae
108 Craton split between North, eastern and western Greenland. Furthermore, the
109 Nagssugtoqidian Orogen has been integrated into the Rae Craton. Thus, 25 non-overlapping
110 geological regions, with 19 having seen sampling for diamond exploration, form the
111 geographic basis for the prospectivity methodology (Figure 1).

112

113 **Regional diamond prospectivity modelling**

114

115 **Prospectivity based on sampling history**

116

117 Sampling history can be treated quantitatively and is a useful metric in determining the
118 completeness and results of diamond exploration. The number of onshore samples taken for
119 the purpose of diamond indicator testing (including diamond-only samples) was counted for
120 each prospectivity region and the numbers of samples which contained diamond indicator
121 minerals (DIM) were compiled. The criteria used to score each region based on sampling
122 history are described in Table 1. The method is based on the principle that regions where a
123 high proportion of samples return positive visually-identified indicator minerals are favoured
124 over those with low recovery success. Furthermore, under-sampled areas provide more
125 opportunity for new discoveries and are therefore favoured over heavily sampled regions. The
126 cut-offs for sampling density follow the scale definitions of McMartin and McClenaghan
127 (2001) and are described in Table 1 in addition to definitions of relative indicator recovery
128 success. Combining sample density with sample success generates a score (Table 1) which
129 can be applied to each region. Some regions have seen no diamond exploration, and so in
130 order to score sampling history in as consistent a geological context as possible, unsampled

131 regions have been scored as follows. Regions, such as the Cenozoic, which have seen no
132 diamond indicator sampling for geological reasons are assigned a score of 6 (consistent with
133 Hutchison, 2012 and 2018b). Whereas regions which have sound geological reasons to be
134 prospective, and yet have not been sampled due to inaccessibility, are assigned a score of 5.

135

136 **Prospectivity based on geological age**

137

138 In order to be exploited economically, diamondiferous bodies must be close to or at surface.
139 Transported material such as glacial sediments, which are common in parts of Greenland,
140 provide impediments to the discovery of primary bodies. However, it is the overlying solid
141 geology that can provide the biggest impediment to economic extraction. Hence, in order to
142 assess the likelihood that diamondiferous rocks will be present at or near the surface, it is
143 important to understand both the likely age of intrusion, based on the known ages of
144 diamondiferous rocks elsewhere, and the ages of the country rocks in the area of interest. If,
145 for example, the age range of rocks in a region is younger than any known diamondiferous
146 rock, then it would be expected that any diamondiferous bodies present would be covered,
147 possibly with kilometres of rock.

148 Ranges of ages of Greenland's 25 unique geological regions are shown graphically in
149 Figure 2, with data sources referenced in Hutchison (2022). The wide range of ages (2.86
150 Gyr) of intrusive events giving rise to diamond-prospective rocks are provided in Figure 2 for
151 context. It is evident that the four main phases of intrusion of diamond-prospective rocks,
152 Jurassic, Ediacaran (Neoproterozoic), Ectasian (Mesoproterozoic) and Orosirian–Stratherian
153 (Paleoproterozoic), postdate many of the rocks at surface in Greenland, certainly all of the
154 cratonic blocks. Furthermore, only four of Greenland's regions (the Cenozoic Basins,
155 Kangerlussuaq Basin, Nuussuaq Basin and the North Atlantic Igneous Province) entirely post-
156 date Greenland's Jurassic diamondiferous kimberlitic rocks.

157 With age ranges of geological regions established, and a knowledge of the ranges of
158 ages of diamond-prospective rocks, a scoring mechanism can be established which allows
159 approximately similar numbers of regions to be assigned to each score. The established
160 method with six classifications is described in Table 1.

161

162 **Prospectivity based on lithosphere characteristics**

163

164 Mantle lithosphere thickness imposes the strongest control on the formation of diamonds
165 (Haggerty, 1994), and overlying crustal weaknesses, often driven by sharp changes in
166 lithosphere thickness, impose the strongest controls on diamond emplacement to the Earth's
167 surface (Helmstaedt and Gurney, 1995; Haggerty, 1999). Cratonic regions of the Earth are
168 typically characterized by thick, cold and old mantle lithosphere that provides the conditions
169 required for diamond formation (Haggerty, 1994; Pearson et al., 2021). Therefore, diamond
170 explorers favour cratonic regions. While cratonic nuclei are the foci of diamond exploration
171 (Pearson et al., 2021) the edges of cratonic regions or craton–craton terrane boundaries are
172 often prospective because they allow diamond-hosting rocks to reach the surface more readily
173 (Helmstaedt and Gurney, 1995).

174 Geothermobarometry of mantle xenoliths variously provide maximum source depths
175 of 215 km (Maniitsoq / Sarfartoq; Sand et al. 2009) and 195 km (Sarfartoq; Hutchison and
176 Frei. 2009), and Larsen and Rønsbo (1993) determined source depths for garnet lherzolites at
177 145–165 km for Sarfartoq and Sisimiut, and 220 km for the Maniitsoq area. Wittig et al.
178 (2010) provide a review of mantle thickness for the whole of West and South-West Greenland
179 with the deepest (> 220 km) mantle centred on Sarfartoq and Kangerlussuaq. Mineral
180 chemical estimates of mantle lithosphere thickness compare favourably to geophysical
181 measurements of the current lithosphere. They are most consistent with Model 2 of depth to
182 the lithosphere / asthenosphere boundary using a method of thermal isostasy of Artemieva

183 (2019). Hence this model is used as the reference framework for prospectivity in this work.
184 The seismic stations upon which the Artemieva (2019) model relies are reasonably evenly
185 distributed throughout Greenland with between four and six seismic stations per five degrees
186 of latitude for the majority of Greenland, and with the southern tip (south of 65°N) having
187 three stations and the northern coastline (north of 80°N) having two stations. Thus while
188 knowledge of the lithosphere thickness in the north of Greenland is anticipated to have more
189 uncertainty, it is only marginally so compared to the rest of the country. Most likely a more
190 impactful influence on uncertainty derives from the distance to earthquake-generating
191 subduction zones, which is similar country-wide.

192 It is notable that known intrusive events of diamond-prospective rocks in Greenland
193 span 2.86 Gyr (Figure 2), which would suggest that different ages and locations of Greenland
194 intrusives may have witnessed different mantle lithosphere conditions over time. Changes
195 may have occurred as a consequence of delamination leading to modified cratons (Pearson et
196 al., 2021), such as seen in Wyoming. However, comparison of the current mantle lithosphere
197 (Artemieva, 2019) and contemporary mantle lithosphere through studies of mantle xenoliths
198 (e.g. Sand et al., 2009 and Wittig et al., 2010) do not provide evidence for delamination at
199 least in western Greenland. Whereas, the Caledonian orogeny may have caused delamination
200 of what is now thin mantle lithosphere (Figure 3; Artemieva, 2019) in east Greenland.

201 For this study, the vertical extents of the mantle lithosphere under Greenland have
202 been subdivided into polygons reflecting the depth ranges of 25–75, 75–125, 125–175, 175–
203 225 and 225–275 km using contours from Artemieva (2019; Figure 3). The two deepest
204 subdivisions lie within the diamond stability field in the mantle lithosphere and the two
205 shallowest subdivisions are outside the diamond stability field. The central subdivision, 125–
206 175 km covers the range over which diamond may or may not be stable under mantle
207 conditions depending on the geotherm. The intersection between each lithosphere polygon
208 and each geological region has been calculated, providing an area in square kilometres for

209 each depth range and each region. This allows the relative proportion of each depth range for
210 each region to be calculated and subsequently an average depth to the lithosphere–
211 asthenosphere also to be calculated. Each region is subsequently assigned a numerical score
212 from 1 to 5, where 1 represents the thickest lithosphere (most diamond-prospective) and 5 the
213 thinnest (Table 1). Scores are attributed to depth ranges to generate an approximate Gaussian
214 distribution (only slightly skewed towards thick lithosphere) among Greenlandic regions.

215

216 **Combined prospectivity**

217

218 For each geological region, the scores for each of the three criteria of age, sampling history,
219 and underlying lithosphere thickness are summed. The regions are ordered or ranked 1st, 2nd
220 equal, 4th equal, and so on, resulting in twelve ranked groups. Each group is subsequently
221 incrementally assigned a category number with 1 being the most prospective and 12 being the
222 least prospective.

223

224 **Mantle mineral modelling**

225

226 Aside from diamonds themselves, mineral chemical characteristics are the single most
227 important criteria, where available, for identifying diamond prospectivity of the deep Earth
228 below any given near-surface location. However, only 44 % of Greenlandic samples reported
229 to have visually-identified indicator minerals have corresponding mineral chemistry data.
230 Consequently, insufficient data exist to allow mineral chemistry to be a statistically robust
231 criteria at the resolution of 25-regions for the quantitative prospectivity described previously.
232 Notwithstanding this shortcoming, abundant mineral chemical data do exist for locations
233 within Greenland and inspection of these data provides useful insights into where mineral
234 chemical techniques yielded exploration dividends and where shortcomings in approaches

235 useful elsewhere may exist. The mineral chemical approach has the advantage that it leads to
236 far fewer false positives and can be queried in a more sophisticated and varied manner than
237 visual indicator mineral identification. Furthermore, the window provided into the lithosphere
238 by mineral chemistry relates to the time of emplacement rather than the present-day picture
239 provided by geophysics. Therefore, the two approaches to understanding diamond
240 prospectivity applied herein – quantitative regional modelling and mineral chemistry,
241 including diamond study – complement each other.

242

243

244 **Results**

245

246 **Historical sampling**

247

248 The large majority (92%) of Greenlandic diamond exploration samples have been taken from
249 unconsolidated sediments with a relatively even split between alluvial sediments from current
250 drainages and glacial material (typically tills). Most diamond exploration in Greenland has
251 focussed on recovery of diamond indicator minerals. Sample sizes appear to have decreased
252 with time with earlier explorers noting 30 to 35 kg alluvial samples being typical. Whereas
253 historical data as a whole reveal of mode of 10 kg for alluvial and glaciogenic samples
254 (Hutchison, 2020a; Hutchison, 2022). In a global diamond exploration context these are small
255 samples, and the most common size range for mineral picking of 0.25 to 0.5 mm has a smaller
256 upper limit than is routinely applied in neighbouring Canada (Hutchison, 2022). However,
257 Greenland appears to present a weathering environment particularly beneficial to the
258 preservation of Cr-spinels as well as less durable minerals including garnets and Cr-diopsides.
259 While all indicator grains disaggregate, particularly Cr-diopside, data demonstrate that the
260 effect on heavy mineral concentrates is that grains appear in smaller size fractions rather than

261 disappearing altogether (Hutchison, 2022). Therefore, it is concluded that sampling strategies
262 in Greenland have usually been adequate, and present a balance between generous sampling
263 and the costs and logistical challenges of exploration.

264 Visually identified indicators overwhelmingly are olivines although these are expected
265 to be largely false positives due to the inability to visually discriminate diamond-associated
266 olivines from others. After olivine, ilmenite is the next most abundant indicator mineral,
267 which itself presents challenges when identifying genuine indicators visually. Cr-diopside,
268 garnet, orthopyroxene and spinel indicator proportions in samples mirror those found in
269 Canada, but it is striking how numbers of garnets, Cr-diopside and orthopyroxenes are very
270 considerably more abundant away from source than in chemically weathered environments
271 such as Australia. In Greenland, the range of ubiquitous mantle minerals found in diamond-
272 prospective rocks genuinely can be used as pathfinders considerably far from source, provided
273 that carefully chosen sample sites are identified.

274

275 **Regional prospectivity modelling**

276

277 The results of prospectivity analysis in terms of the quantitative ranking of geological regions
278 based on sampling density and success, ages of surface rocks and underlying lithosphere
279 characteristics, and, separately, in terms of diamond recovery and the re-assessment of
280 mineral chemical data using standardised datasets, are discussed in the following.

281 Results for individual criteria and total rankings contributing to quantitative
282 prospectivity analysis are shown in Table 2.

283

284 **Results of sample success scoring**

285

286 Results of sampling history are provided in Figure 4, tabulated in the supplementary data
287 appendix (Supplementary Table 1). Regionally, sampling density has been low, with no
288 Greenlandic region experiencing what would be considered local sampling density (more than
289 one sample per 4 km²). The NAC of western Greenland has the highest average sample
290 density of 2292 samples per 100 x 100 km area.

291 The Inglefield Orogenic Belt distinguishes itself by having a 100% sampling success
292 rate. However, this is due to only one sample being collected, and being indicator-positive.
293 This statistical bias is handled in the context that sample scoring is only one of three metrics,
294 and, as shall be discussed later, empirical modifications can be applied to final scoring where
295 considered justifiable. The other top score from sample success is assigned to the Franklinian
296 Basin, where 82% of samples are indicator-positive. This result is contributed to most
297 significantly by the visual identification of orange and red garnets in surface sediment
298 samples (Hutchison, 2020a, 2022) in the vicinity of the inlier designated as part of the Rae
299 Craton (Nutman et al., 2019). The most statistically robust high scores (value of 2) were
300 found for the Gardar Province, Ketilidian Orogen, NAC in western and eastern Greenland and
301 the Rae Craton in western Greenland.

302

303 **Results of age dependent scoring**

304

305 As may be expected, the top score exclusively falls to all Greenland's exposed cratonic
306 nuclei, namely the NAC in western and eastern Greenland and the Rae Craton in western,
307 eastern and North Greenland. While not discriminated between, in terms of scoring, the NAC
308 of eastern Greenland and Rae Craton of North Greenland distinguish themselves as having no
309 reported rocks younger than the oldest of any known diamond-prospective rock in Greenland.
310 However, given that this oldest occurrence is the 2664 Ma Singertat Carbonatite which has no
311 known diamondiferous rocks associated with it to date, the distinction is perhaps academic.

312 Other regions which score well due to age are the Caledonian basement, Inglefield Orogenic
313 Belt, Karrat Basin, Ketilidian Orogen and the small Prøven Igneous Complex of North-West
314 Greenland.

315 It is noteworthy, however, that since the age-dependent scoring is focused on primary
316 diamond deposits, the low score for the Nuussuaq Basin contrasts with the prospectivity of its
317 sedimentary successions as sources of re-worked diamonds as palaeoplacers (Hutchison,
318 2022).

319

320 **Results of lithosphere thickness scoring**

321

322 Due to the prominent, thick mantle lithospheric keel under West Greenland, the NAC and Rae
323 Craton of western Greenland score best for lithospheric prospectivity. This high ranking is
324 consistent with the abundant deep-sourced mantle xenolith data from western Greenland (e.g.
325 Sand et al., 2009; Wittig et al., 2010), and the known occurrences of diamond, from
326 Pyramidefjeld to Svartenhuk Halvø (both extents being consistent with a depth of 200 km to
327 the lithosphere / asthenosphere boundary following the model of Artemieva, 2019). High
328 rankings are also achieved by the basins surrounding these cratons, such as in the Disko Bay
329 area, the Inglefield Orogenic Belt, and the Ketilidian Orogen and Gardar Province (scoring 2).
330 However, perhaps surprisingly, northern Greenland also scores well with the Independence
331 Fjord and Franklinian Basins both scoring 3. This is a consequence of a relative thickening of
332 the mantle lithosphere moving increasingly north from the Humboldt Glacier (80°N) with its
333 maximum corresponding with the small inlier of rocks attributed to the Rae Craton in North
334 Greenland (Nutman et al., 2019).

335

336 **Overall ranking**

337

338 All 25 regions ranked from 1st to equal 22nd place give the 12 discrete ranking categories
339 previously described and these are used to colour-code the prospectivity map of Greenland
340 (Figure 5). The Rae Craton and NAC of western Greenland distinguish themselves by having
341 the highest modelled diamond prospectivity rankings. This derives from the good success in
342 visually identified indicator mineral recovery, including diamonds (albeit with many samples
343 deriving from already identified bodies), the age of the rocks and also the thick mantle
344 lithosphere keel lying well within the diamond stability field. The next best score, however, is
345 assigned to the Inglefield Orogenic Belt. The high scoring derives from good indicator
346 recovery from very low density sampling, but also the old age of the rocks and the thick
347 lithospheric keel under this small, northern region of Greenland. Notable, with a final score of
348 3 are the Ketilidian Orogen and NAC of eastern Greenland. The Ketilidian is known for
349 strongly-prospective indicator minerals and known ultramafic lamprophyres and its ranking is
350 boosted by sitting on the edge of the thick mantle keel of western Greenland and being
351 comprised of relatively old rocks. The ranking of the NAC of eastern Greenland falls below
352 the NAC of the west due to thinner lithosphere (although still within the diamond stability
353 field). The Rae Craton of eastern Greenland (scoring 5) falls quite far below its counterpart in
354 western Greenland due to considerable portions falling within the thin, likely strongly
355 delaminated lithosphere (Figure 3) affected by the Caledonian Orogeny. The Rae Craton of
356 North Greenland scores poorer still (scoring 6) but this region is pulled dramatically
357 downwards by the absence of any sampling having been conducted in this small region.

358

359 **Indicator mineral chemistry**

360

361 Acquisition of mineral chemical data is costly and time consuming. However, the process of
362 fieldwork, sampling, transporting, processing and picking indicator minerals is extremely
363 costly. Hence, acquiring mineral chemical data is proportionally not a large part of an

364 exploration budget. Nevertheless, mineral chemical determination has often been neglected
365 among Greenland diamond exploration with less than half of visually identified indicator-
366 positive samples being subjected to mineral chemical testing (Hutchison, 2022). Where
367 mineral chemical data are available, they provide valuable insights into diamond prospectivity
368 as demonstrated for the Sarfartoq area by Grütter and Tuer (2009), and as discussed in the
369 following.

370

371 **Pyroxene chemistry**

372

373 Mineral chemical data have been derived from diopside-hedenbergite grains from the NAC
374 and Rae Cratons in western Greenland, the Ketilidian Orogen, and the Karrat Basin (which
375 lies north of the Nuussuaq Peninsula; Figure 1). Figure 6 shows their compositions in terms of
376 Al_2O_3 and Cr_2O_3 content. Two Rae Craton outliers contain over 13 wt% Al_2O_3 and one has
377 over 15 wt%, and a further two outliers have Cr_2O_3 over 5 wt% and are not plotted in Figure
378 6.

379 Clinopyroxenes from the NAC of western Greenland express compositions well
380 constrained to within the garnet peridotite field and rarely with Cr_2O_3 above 3 wt%. The core
381 of NAC compositions is constrained between approximately 1 and 2.5 wt% Al_2O_3 with
382 variable Cr-content within the garnet peridotite field. However, there is also a small
383 discernible trend of increasing Al-content into the spinel lherzolite field. In contrast, grains
384 from the Rae Craton show a wider range of composition extending above 5 wt% Cr_2O_3 in rare
385 cases, and similar to the diversity of compositions seen in Canada (Northwest Territories
386 Geological Survey, KIDD/KIMC, 2017). Wide compositional variability reflects both a range
387 of depths of origin and also bulk mantle chemistry. The trend through the spinel lherzolite
388 field and beyond with increasing Al content is more marked in Rae Craton samples, than the
389 NAC, and similar to Baffin Island samples from the moderately to poorly diamondiferous

390 Brodeur Peninsula (Northwest Territories Geological Survey KIDD/KIMC, 2017) and
391 Chidliak (Pell and Nielson, 2008). Ketilidian Orogen clinopyroxenes describe two distinct
392 groups within the garnet peridotite field, being a high Cr group (with Cr₂O₃ between c. 2-3
393 wt%) with Al₂O₃ constrained between 0.7 and 1.5 wt%, and a low Cr group (with Cr₂O₃
394 below 2 wt%). The low Cr group, as also evident in Rae Craton samples, extends across all
395 Al₂O₃ concentrations between c. 0.3 wt%, into the spinel lherzolite field and beyond to over
396 10 wt% Al₂O₃. While the Brodeur Peninsula kimberlites in Canada show the same shallowing
397 depth trend as apparent particularly in Rae Craton samples, encouragingly from a diamond
398 prospectivity perspective, the Chidliak diamondiferous kimberlites show the same strong
399 variability in Cr-content within the garnet peridotite field as Greenlandic NAC, Rae Craton
400 and Ketilidian Orogen samples.

401 Further to general chemical trends in unclassified pyroxenes as described previously,
402 single clinopyroxene grains can also provide opportunities for determination of temperature
403 and pressure (and, hence depth) of equilibration within the mantle. The methodology of
404 Sudholz et al. (2021a) applies their revised Cr-in-clinopyroxene barometer and relies on the
405 enstatite-in-clinopyroxene thermometer of Nimis and Taylor (2000). Since clinopyroxene
406 grains recovered from surface sediment samples have no demonstrable genetic association
407 with accompanying mineral grains, and can have a range of sources throughout the crust and
408 mantle, Sudholz et al.'s (2021a) methodology provides very rigorous filters (following
409 methods of Grütter, 2009 and Zibera et al., 2016) to ensure derivation from garnet
410 lherzolites.

411 The database of Hutchison (2020a) provides 16 563 analyses of Greenlandic
412 clinopyroxenes which pass criteria described by Hutchison (2020b) as acceptable analyses.
413 The method of Sudholz et al. (2021a) has been applied to all data, both from known
414 kimberlites and aillikites, and surface sediments, and rigorous filters result in 956 mineral
415 grains providing defensible pressures and temperatures of origin. All accepted grains derive

416 from the North Atlantic and Rae Cratons of western Greenland, and the Ketilidian Orogen.
417 Geothermobarometry data are presented in Figure 7 plotted as temperature against depth, and
418 with mantle geotherms of Hasterok and Chapman (2011) and the diamond / graphite phase
419 transition of Day (2012) for reference.

420 North Atlantic Craton garnet lherzolite clinopyroxenes derive from locations covering
421 the whole extent of the Craton on the west coast. Sub-100 km origin clinopyroxenes (outside
422 the diamond stability field) are sourced from the same geographic extent (reflecting being
423 accumulated on ascent from melts sourced at a wide range of depths). However, with three
424 exceptions from a Tikiusaaq sample (up to 199 km, 65.2 kbar, 1352 °C, Hutchison 2020a
425 sample ID 459144) all clinopyroxenes from over 160 km in depth come from the northern
426 extent of the Craton on either side of the Maniitsoq (Sukkertoppen) Icecap. From latitude
427 61°N to 67°N, the thickness of mantle lithosphere sampled increases (from 57 km to 176 km),
428 with the maximum depth increasing, and the minimum depth decreasing as clinopyroxenes
429 derive from more northern latitudes. At the large scale, there is no clear trend in geographic
430 source among clinopyroxenes derived from over 200 km deep, aside from the fact that the
431 super-deep samples (over 220 km in origin) all come from Garnet Lake. The deepest
432 clinopyroxene discovered in Greenland by this method is calculated to derive from 228 km
433 (74.5 kbar, 1272 °C, from kimberlite sample MHG9_6, Hutchison, 2020a).

434 Rae Craton clinopyroxene data scatter around a slightly wider range of reference
435 mantle geotherms, both cooler and warmer than North Atlantic Craton clinopyroxenes but the
436 difference is minor. Aside from an unremarkable sample from the Disko Bay area within the
437 graphite stability field at 116 km depth of origin, all Rae Craton samples derive from 35 km
438 of the southern boundary with the North Atlantic Craton and sample 164 km of thickness of
439 mantle. Many samples lie respectably within the diamond stability field with the deepest
440 being sourced from 222 km (72.6 kbar, 1312 °C, Hutchison 2020a sample ID 111735).

441 The samples from the Ketilidian Orogen revealing single clinopyroxene
442 geothermobarometry data cover the northwestern part of the Orogen, from Narsarsuaq (Johan
443 Dahl Land) to almost as far west as Kobberrminebugt (south of Grønnedal). There is no
444 geographic distinction between the clinopyroxenes which express warm mantle geotherms (40
445 to 50 mWm⁻²) compared to the deeper sourced (over 146 km depth of origin) mineral grains
446 which derive from cooler (35 to 40 mWm⁻²) geotherms more favourable to diamond
447 formation. However, the large majority of deep sourced grains derive from Johan Dahl Land
448 samples. Among these are the deepest sourced Ketilidian Orogen grain (Hutchison 2020a
449 grain ID 3941 from 208 km, 68.0 kbar, 1225 °C) which derives from the same sample –
450 Hutchison (2020a) sample 100071 – which also produced 108 km and 193 km-sourced
451 clinopyroxenes. All these clinopyroxenes derive from comfortably within the diamond
452 stability field and emphasise the significance of the Ketilidian Orogen on par with the deeper
453 portions of the North Atlantic and Rae Cratons. Recent diamond exploration in a portion of
454 Johan Dahl land and near to Narsaq (Bernstein et al., 2025) failed to reveal diamond indicator
455 minerals. However, their findings, restricted to fairly small geographic areas (15 km radius),
456 include previously unreported UML dykes which demonstrate the variability of diamond
457 prospective bodies in comparison to known South Greenland breccias (e.g. Upton et al., 2006)
458 and the impact that alteration can have on preservation of indicator minerals.

459 Orthopyroxene does not commonly survive in diamond exploration samples
460 worldwide. However, a statistically significant number (1202) of good-quality mineral
461 chemical analyses for orthopyroxene are available in Hutchison (2020a) with 817 being
462 considered genuine indicators following Ramsay and Tompkins (1994). All orthopyroxene
463 grains of interest for diamond exploration with reported mineral chemistry data derive from
464 the NAC and Rae Cratons and the Ketilidian Orogen. Classification following Ramsay and
465 Tompkins (1994) show distinct difference between orthopyroxenes from the Rae Craton,
466 compared to western Greenland's NAC and grains from the Ketilidian Orogen (Hutchison,

467 2022). While Rae Craton grains generally are less Mg-rich, falling into megacryst and
468 eclogitic fields, NAC and Ketilidian Orogen grains have compositions consistent with
469 peridotites, particularly those from diamondiferous garnet lherzolites. While Mg-
470 compositions reflect different dominant mantle compositions, increasing Al-content reflects
471 shallowing depth. Hence the Rae Craton samples demonstrate a range in source depths, into
472 non-diamond prospective, shallow depths, whereas NAC compositions are more consistently
473 deep. The Ketilidian Orogen samples express two distinct compositional fields, both deep-
474 sourced with the shallower consistent with diamondiferous lherzolites and the deeper, or at
475 least more depleted, consistent with harzburgites. Canadian samples (Northwest Territories
476 Geological Survey KIDD/KIMC, 2017) reveal both diamond-associated compositions, but
477 also a range of higher Al-content orthopyroxenes into the shallower spinel lherzolite field not
478 seen in Greenlandic samples. Away from the highly diamond-prospective Canadian Lac de
479 Gras area, the compositional range to more Fe-rich orthopyroxenes is also mirrored in western
480 Greenland's Rae Craton samples.

481

482 **Garnet chemistry**

483 Garnet is considered a particularly useful mineral for diamond exploration because its large
484 compositional variability can often allow attribution to very specific geological environments
485 associated with high pressures within the mantle lithosphere (Grütter et al., 2004). In contrast
486 to warmer climates, arctic environments such as in Greenland or Canada allow garnets to
487 survive as an indicator mineral distal from its source rock (Hutchison, 2022).

488 Mineral chemistries have been obtained from pyrope-almandine–grossular garnets
489 from five regions (Hutchison 2020a), namely the NAC and Rae Cratons in western
490 Greenland, the NAC in South-East Greenland, the Nuussuaq Basin (samples which derive
491 from western Rae Craton basement rocks), and the Ketilidian Orogen. Garnet mineral
492 chemistry is shown in terms of Ca and Cr content in Figure 8, compared with Canadian data

493 from northern Baffin Island (Rae Craton at the Brodeur Peninsula) and elsewhere in the
494 Northwest Territories and Nunavut (Northwest Territories Geological Survey, KIDD/KIMC,
495 2017). Data are plotted according to CaO and Cr₂O₃ content and subdivided following the
496 methodology of Grütter et al. (2004). The spread of mineral chemistry, among both mantle-
497 derived and other garnets is wider for the Rae Craton samples compared to the NAC samples.
498 All of the Rae Craton, NAC, Ketilidian Orogen and Nuussuaq Peninsula garnet compositions
499 show strong and convincingly G9 lherzolitic compositional trends. Rae Craton, NAC and
500 Nuussuaq Peninsula garnets from western Greenland also yield many compositions residing
501 in the diamond-prospective G10 field. Furthermore, chemical analyses of a suitably high
502 quality (as determined by electron microprobe) and with measured Mn-contents, allow
503 definitive classifications in the G10D (diamondiferous) field for Rae Craton and NAC
504 samples. Very few Brodeur Peninsula (Rae Craton of Canada) garnets fall within the G10
505 (and G10D) fields (Figure 8). In this regard, Canadian samples of the Brodeur Peninsula most
506 closely mirror the small number of Ketilidian Orogen garnets, which express compositional
507 variability in the G9 lherzolitic field. The Greenlandic garnets from the NAC and Rae Cratons
508 of western Greenland, with the presence of G10 compositions, therefore reflect a more
509 diamond-prospective mantle source than on the Canadian side of the Rae Craton. Similar
510 compositional ranges into the G10 field to Greenland's NAC, Nuussuaq Peninsula and Rae
511 Craton in the west, can be found further south on Baffin Island in garnets from the
512 diamondiferous aillikites at Chidliak (Pell and Neilson, 2012). Greenlandic garnets compare
513 favourably with those presented in the Canadian database of Northwest Territories Geological
514 Survey, KIDD/KIMC (2017) from the diamond-mining fields of Ekati and Diavik.

515 Particular importance is placed on the role of G10 composition garnets as an indicator
516 of diamond prospectivity. Certainly, there is a strong association between G10 composition
517 garnets and known diamondiferous bodies, including those which are mined. However, G9,
518 lherzolitic garnets can very much also be associated with diamondiferous bodies, such as at

519 Diavik (Moss et al., 2018), Victor (Stachel et al., 2017) and Forte à la Corne (Banas et al,
520 2025). Therefore, aside from the significance of G10 garnets, the presence of G9 garnets
521 among Greenland samples can be taken as a positive for diamond prospectivity, particularly
522 due to the shared geological history with Canada.

523 Garnet compositions also lend themselves well to diamond-provenance assessment
524 using the Ni-in-garnet thermometer of Griffin and Ryan (1995), refined most recently by
525 Sudholz et al. (2021b). As for G-classifications following Grütter et al. (2004), inspection of
526 Hutchison (2020a) data shows that Greenlandic garnets perform well in terms of diamond
527 prospectivity by this method.

528

529 **Ilmenite chemistry**

530

531 Acceptable mineral chemical data have been obtained for 47 722 ilmenite grains from
532 Greenlandic samples. A total of 44 845 have indicator mineral compositions following Wyatt
533 et al. (2004) – i.e., only 2877 grains, 6%, fall in Wyatt et al.’s (2004) non-kimberlitic field –
534 with 43 121 being in Wyatt et al.’s (2004) kimberlite field and the remainder being classed as
535 with intermediary compositions..

536 Ilmenite chemical compositions shown in Figure 9 are plotted according to TiO₂ and
537 MgO. This diagram aims to discriminate ilmenites with a potential kimberlitic association
538 from so-called intermediary compositions and those not consistent with a kimberlite source.
539 Samples from the NAC and Rae Cratons of western Greenland, and from the Nuussuaq Basin
540 (samples presumably derived from re-worked Rae Craton rocks) all show high proportions of
541 ilmenites falling clearly within the field associated with kimberlites from worldwide. The
542 Ketilidian Orogen samples are few in number and less convincingly diamond-prospective by
543 this method, with only one grain falling within the kimberlite field. Similar to the observation
544 for garnet chemistry, the spread of mineral chemistry among both kimberlite-associated and

545 other ilmenites is wider for the Rae Craton samples compared to the NAC samples. Bernstein
546 et al. (2025) made similar findings amongst Ketilidian origin ilmenites, and it is hypothesised
547 that ilmenite compositions may have been affected by metamorphism among these rather
548 older (Proterozoic; Figures 1 and 2) southern Greenland diamond-prospective bodies.

549 It is evident when comparing Figure 9a and 9b that among Canadian ilmenites, the
550 marginally diamondiferous-Brodeur Peninsula samples show a very slightly lower Mg and
551 higher Ti compositional range than the more diamondiferous Canadian samples which include
552 those from the Ekati and Diavik mining districts. This regional Canadian trend is mirrored
553 very closely by the western Greenlandic NAC ilmenites to the full extent of their high-Mg
554 range (Greenlandic samples are, in fact, more Mg-rich). With a wider ilmenite compositional
555 variability, western Greenland's Rae Craton samples also comfortably completely encapsulate
556 ilmenite compositions from Canada's diamond-mining districts, including the Lac de Gras
557 area.

558 In addition to providing valuable insights into the likely derivation of ilmenites from
559 kimberlites or related rocks, ilmenite compositions can also indicate the likely preservation of
560 diamonds should they be present as xenocrysts in ilmenite-bearing rocks. Diamond can be
561 chemically degraded in oxidising conditions and so by inspecting the relationship between
562 ferric (Fe^{3+}) iron and Mg in ilmenites, ambient oxidation can be inferred. In some cases, it has
563 been demonstrated that oxidations calculated in this way has a correlation with diamond grade
564 and morphology (Gurney and Zweistra, 1995), although this is not universally the case
565 (Robles-Cruz et al., 2008). Nevertheless, ilmenite composition at least remains useful as a
566 qualitative indicator of the environment within which diamonds have been transported.

567 All 54 777 good-quality chemical analyses of ilmenite in Hutchison (2020a), and from
568 Northwest Territories Geological Survey, KIDD/KIMC (2017) have had cation concentrations
569 of ferrous and ferric iron calculated by charge balancing to achieve 2 cations per 3 anions.
570 Each ilmenite chemical formula has then been re-cast to oxide percentage abundances by

571 mass to achieve assessments of FeO and Fe₂O₃ concentrations. These data have been plotted
572 against measured MgO contents as shown on Figure 10, showing ranges of inferred diamond
573 preservation following Gurney and Zweistra (1995).

574 Compositions of ilmenites derived from the Nuussuaq Peninsula (with a likely Rae
575 Craton source) match those from diamond-marginal kimberlites of the Canadian Rae Craton
576 in northern Baffin Island (Northwest Territories Geological Survey, KIDD/KIMC, 2017).
577 However, western Greenlandic Rae Craton samples, and particularly those from the NAC also
578 reflect the highest degrees of preservation. This preservation index is seen also among
579 Chidliak diamondiferous kimberlites (Pell and Nielson, 2008), and matching the NAC
580 compositions, is strongly seen among ilmenites from the diamond-mining districts elsewhere
581 in Canada (also from Northwest Territories Geological Survey, KIDD/KIMC, 2017). For
582 indicator mineral-classed ilmenite compositions (as for other indicator minerals) Rae Craton
583 samples show the widest range in ilmenite compositions recovered in Greenland. This range
584 reflects kimberlite oxidation values which, if a useful metric in this context, would cause the
585 whole range of diamond survival from full resorption to complete diamond preservation.

586

587 **Spinel chemistry**

588

589 Spinel compositions compiled in Hutchison (2022a) have been classified according to major and minor
590 element compositions adapted from Ramsay (1992) as described in Hutchison (2020b).

591 Attribution as indicator minerals for diamond potential follows this classification where
592 aluminospinel-(Mg) ± Ti, Cr and gahnite-(Fe), and all chromites apart from end-member
593 aluminochromite are all classed as indicators – other compositions are excluded. Among the
594 indicator spinels, the majority are chromites (13 860 grains). In terms of provenance, almost
595 equal numbers of spinel indicator minerals were reported from the western extents of the
596 NAC (6954 grains) as the Rae Craton (6808 grains). However, the abundance of different

597 spinel compositions differs significantly. While 34% of NAC indicator spinels are Ti-bearing,
598 this proportion is much higher in Rae Craton samples (62%). In contrast, the proportion of Al-
599 bearing chromites is considerably lower amongst Rae Craton samples (constituting 3%)
600 compared to making up 14% of NAC indicator spinels.

601 Indicator spinels have been further subdivided according to the methodology of
602 Grütter and Apter (1998). A total of 111 chromites with compositions consistent with
603 chromite inclusions in diamond (designated SP-CID or CID in the database) have been
604 identified, all from the western parts of the NAC and Rae Craton. This makes them rare, but
605 they are significantly more abundant from the NAC (1.2% of all indicator spinels) compared
606 to the Rae Craton (0.4%).

607 Further chemical discrimination using only spinels that were determined to be
608 indicator minerals has the potential to provide a more specific attribution to host rocks. Figure
609 11 shows Cr relative to Cr + Al cations plotted against Fe^{2+} relative to $\text{Fe}^{2+} + \text{Mg}$ cations
610 where Fe has been attributed to both ferric and ferrous oxidations states based on cation
611 calculations and charge balance (i.e., projected onto the oxidized prism of Mitchell, 1986).
612 This diagram allows comparison with spinels from worldwide locations associated with
613 kimberlites, xenoliths in kimberlites and as inclusions in diamond (Mitchell, 1986). The
614 numbers of chromites consistent with inclusions in diamond according to both this criteria
615 (the labelled field in Figure 11) and Grütter and Apter's (1998) separate methodology is
616 small. Whereas Grütter and Apter's (1998) methodology identifies three times the proportion
617 of chromite inclusion in diamond compositions from the NAC compared to the Rae Craton, in
618 contrast, Mitchell's (1986) method attributes almost all diamond-association chromites as
619 being from the Rae Craton (Figure 11). For the Ketilidian Orogen, it is interesting to note that
620 there appear to be two distinct groups of compositions, being a trend towards both chromium
621 and magnesium-rich compositions, and a Cr-poor and ferrous Fe-poor group. NAC and Rae
622 Craton spinel compositions also express a Cr-poor and ferrous Fe-rich group, outside

623 kimberlite-associated compositions, which possibly reflects serpentinite and greenschist
624 origins such as from the Tartoq Greenstone Belt in the southern NAC (van Hinsberg et al.,
625 2018).

626 Comparison with Canadian spinels (Figure 11), both from the Brodeur Peninsula of
627 northern Baffin Island (the closest part of the Rae Craton in Canada with known
628 diamondiferous kimberlites) and elsewhere in Nunavut and the Northwest Territories
629 (Northwest Territories Geological Survey, KIDD/KIMC, 2017) show good comparisons with
630 Greenlandic indicators. Inspection of the distribution of 99% of Canadian samples, some of
631 which derive from the vicinities of the world-class diamond mines of Diavik and Ekati, shows
632 that a similar very low proportion of inclusion-in-diamond spinel compositions is evident in
633 Canada as Greenland. Therefore, a rarity of CID spinels should not necessarily be taken as an
634 indication of reduced diamond prospectivity.

635 It is unfortunate that while spinel is an abundant indicator mineral, and certainly a
636 useful tool, major and minor element chemistry does not allow for a discrimination between a
637 diamond-prospective and nondiamond-prospective source as robustly as for other some
638 indicator minerals. Methods based on trace element compositions (such as Co, Cu, Ga, Mn,
639 Nb, Ni, Sc, Ti, V and Zr; Griffin and Ryan, 1995) yield much more definitive diamond-
640 prospective associations than for major and minor elements. Although this method has been
641 used with success elsewhere on the NAC in Scotland (Hutchison et al., 2018), and is
642 considered to be a fairly standard procedure for the larger companies overseas, trace element
643 compositions of spinels have not been reported during diamond exploration in Greenland.

644

645 **Diamonds**

646

647 Diamond survives chemical and physical degradation better than any other mineral derived
648 from diamond-hosting rocks. Consequently, with increasing distance from host rocks,

649 diamond increasingly becomes the most likely diamond-associated mineral to be recovered
650 from exploration samples. Only eight samples of transported sediment recovered during
651 Greenland diamond exploration have proven to contain diamonds (with three of those being
652 palaeochannel mini-bulk samples of several hundreds of kg). However, diamond recovery
653 from transported or in situ rocks known or suspected to be kimberlitic is much more common
654 (176 samples reported in Hutchison, 2022). The craton-sourced diamond samples in
655 Greenland extend from 61.4°N at Pyramidefjeld, north of Ivittuut (Grønnedal) to 69.9°N at
656 Anap Nunaa on the north side of Disko Bay. Diamonds occur in six discrete areas coincident
657 with most of the clusters of kimberlites and ultramafic lamprophyres known in western
658 Greenland.

659 The largest numbers of microdiamonds and macrodiamonds, and the largest stones,
660 derive from the most intensely studied bodies, being the Garnet Lake kimberlite / aillikite sill
661 complex (NAC of western Greenland; Hutchison and Frei, 2009) and the cluster of aillikite
662 dykes at Qeqertaa (Rae Craton; Bernstein et al., 2013). Garnet Lake produced the sample with
663 most macrodiamonds (1096; Hutchison, 2020a) and Qeqertaa the sample with most
664 microdiamonds (1452; Hutchison, 2020a). Notable stones from Garnet Lake are a 2.39 metric
665 carat diamond from a 47-tonne sample and 2.51 metric carat (8.9 x 8.2 x 7.5 mm) from a 160
666 tonne DMS sample taken the following year (Hutchison, 2022).

667 Detailed information on the features and characteristics of Garnet Lake diamonds are
668 discussed in Hutchison and Heaman (2008) and Hutchison and Frei (2009) and are combined
669 with descriptions of the full range of Greenlandic diamonds in Hutchison (2022). Diamonds
670 from southern West Greenland, in the northern part of the NAC and southern Rae Craton have
671 approximately two thirds of stones described as colourless. Most remaining southern West
672 Greenlandic stones are described as grey which may reflect surface frosting hiding a clear
673 interior. Of the 167 stones from central West Greenland in the vicinity of Disko Bay there is a
674 yet higher proportion of colourless stones (83%). Garnet Lake stones are more likely to be

675 octahedral (43%) than the local Sarfartoq average, both of which are lower than the 60% seen
676 from south of the Maniitsoq (Sukkertoppen) Ice Cap, in the area east of the town of
677 Maniitsoq. In contrast, Disko Bay stones are exceptional, in having 90% of stones described
678 as octahedral (Hutchison, 2022). In terms of more marked resorption (rather than surface
679 features) where changes have occurred in the morphologies of the whole diamond, once
680 again, Disko Bay diamonds distinguish themselves. Approximately half of Disko Bay stones
681 show 85 – 95% preservation.

682 The relative abundance of diamonds of varying size is a powerful predictive tool in
683 assessing the economic interest of a diamond deposit (Chapman and Boxer, 2004). Hutchison
684 and Heaman (2008) investigated the size distribution of Garnet Lake diamonds from 425.1 kg
685 of kimberlite from the main Garnet Lake sheet recovered from drill holes and surface
686 samples. The smooth distribution of different diamond sizes was cited as evidence for a single
687 population of stones with little growth of diamond within the kimberlitic melt. The same
688 methodology is applied to subsequently much larger samples of Garnet Lake diamond
689 processing, in addition to data from the Qeqertaa ultramafic lamprophyre, Disko Bay
690 (references in Hutchison, 2022). Size fraction distributions from these expanded data in the
691 context of results from similarly advanced Canadian exploration projects are shown in Figure
692 12. Both Garnet Lake and Qeqertaa microdiamond abundance (diamonds are smaller in size,
693 but more abundant on the left side of the abscissa) compares very well with similar-stage
694 exploration projects from Canada, with Qeqertaa samples being particularly microdiamond-
695 rich. A shallow slope towards larger stones compared to Canadian deposits is particularly
696 pronounced among Garnet Lake microdiamonds. Qeqertaa samples, particularly, show a good
697 consistency between chemically-recovered microdiamonds from mechanically-recovered
698 larger stones, reflecting efficiency in DMS processing. Comparing Garnet Lake and Qeqertaa
699 samples further shows the absence of large stones at Qeqertaa (identified with the largest
700 Qeqertaa diamond being 0.02 metric carats compared to 2.51 metric carats from Garnet

701 Lake). This difference is explained by the larger size of Garnet Lake samples. However, what
702 is also evident is that the Qeqertaa samples show a steeper reduction in the diamond size
703 compared to Garnet Lake. If Garnet Lake recovery efficiency of large stones could be
704 improved to match microdiamond recovery, size distributions would match the best of
705 similar-stage Canadian exploration samples.

706

707

708 **Discussion**

709

710 **Caveats and enhancements to modelling**

711

712 The regional prospectivity modelling presented herein, as for similar studies in Australia
713 (Hutchison, 2012 and 2018b) takes a quantitative approach. Focus is on visually identified
714 indicator minerals, as these remain the primary method for diamond exploration and generate
715 the largest amount of quantifiable data. However, visual determination is imprecise and can
716 lead to false positives and negatives. For example, it is unclear what the chemically untested
717 red and orange garnets (Hutchison, 2020a) reported from the largely under-explored
718 Franklinian Basin of North Greenland, and its associated Rae Craton Inlier, reveal about
719 diamond prospectivity. While mineral chemical data would, ideally, be available for all
720 candidate indicator minerals, cost and time have prohibited this.

721 Numerous factors have an influence on the attractiveness of specific areas, both at a
722 small and large scale and sometimes with considerable effect. Known diamondiferous bodies,
723 favourable mineral chemistry, and anomalous diamond occurrences in surface samples are all
724 positive variables not quantified in the core prospectivity model. Negative factors can be
725 influential, for example, much of Greenland is remote and the cost and benefit considerations
726 of exploration can be heavily influenced by locality. Deep glacial weathering can be

727 detrimental to prospectivity for primary diamond deposits. However, glacial activity results in
728 considerable offshore (quantified by Weidick and Bennike, 2006) and onshore sedimentary
729 successions, having considerable potential for diamond presence. Of particular note in that
730 regard is the Nuussuaq Basin (references in Hutchison, 2022) where, depending on
731 concentration mechanisms, palaeoplacers derived from Rae Craton diamonds may occur.
732 However, the prospectivity modelling is not designed to capture offshore placer diamond
733 deposits because of the bias towards old, rather than young rocks. Reworked deposits are
734 naturally downgraded in the quantitative analysis and must therefore be manually upgraded
735 when considering exploration planning. Therefore, despite the rigour and utility of the
736 prospectivity model, explorers are encouraged to consider less quantifiable variables, with
737 more detailed examples discussed in Hutchison (2022).

738

739 **Un- and under-explored localities**

740

741 Specific observations of under-explored localities include the presence of a single diamond
742 reported from a 28.6 kg sample taken from an in-situ occurrence of metamorphosed
743 ultramafic lamprophyre in the Karrat Basin (71.9°N; Hutchison, 2022). This discovery is
744 anomalous and significant. Unexplored land abounds, even in otherwise well-explored areas
745 with good diamond recovery, such as inland areas close to the Inland Ice both north and south
746 of the Maniitsoq (Sukkertoppen) Ice Cap. The Maniitsoq area has been significantly explored
747 near sea level, particularly at Majuagaa and Søndre Isfjord (Nielsen and Jensen, 2005).
748 However, as Bonow et al. (2006) demonstrate, sea level is not an optimum place to look in
749 western Greenland for more economically prospective parts of a kimberlitic volcanic
750 succession, namely diatreme and crater rocks in pipes.

751 The Ketilidian Orogen and Gardar Province of southern Greenland score well on
752 prospectivity modelling. While indicator minerals are apparently not abundant, this may

753 mirror a similar paucity of fresh indicator minerals seen at Qeqertaa (S. Bernstein, 2022, pers.
754 comm.). Both the Rae Craton at Qeqertaa and the Ketilidian Orogen have seen low grade
755 metamorphism, thus it is hypothesised that these areas may lend themselves less well to non-
756 diamond indicator mineral prospecting than areas of fresher primary bodies such as the NAC
757 of western Greenland. Among known indicator grains from the Ketilidian Orogen and Gardar
758 Province, mineral chemical analyses are encouraging, and Upton et al (2006) reported
759 prospective aillikite diatremes. In fact the southern Greenland ultramafic lamprophyres are
760 considerably distinct in age (Proterozoic), despite perhaps having similar metasomatic origins
761 (Beard et al., 2024), from the succession of Phanerozoic intrusives younging north to south as
762 the Davis Strait expanded from the coast of western Greenland (Larsen et al., 2009). Thus,
763 Ketilidian and Gardar hosted rocks with diamond potential should be considered completely
764 separately from those further to the north. It is also noteworthy that while the basement is
765 relatively young in South Greenland (1.30 to 1.12 Ga Gardar rocks, Upton et al, 2003, intrude
766 into 1.87 to 1.72 Ga Ketilidian host rocks, Henriksen et al, 2009) compared to Greenland's
767 cratonic nuclei, precedent exists among diamondiferous rocks elsewhere in relatively young
768 cratons. For example, the diamondiferous kimberlites in the vicinity of the Wyoming Craton
769 are intruded into 1.8 to 1.4 Ga basement (Carlson et al., 2004). Furthermore, South Greenland
770 does not seem to have experienced the same mantle lithosphere delamination (Artemieva,
771 2019) that the Wyoming Craton has experienced.

772 It is noteworthy that while reports of indicator minerals (referenced in Hutchison,
773 2022) may be spurious due to confusion between submitted samples and laboratory standards
774 (G. Della Valle, 2023, pers. comm.), at Skjoldungen (Figure 1) a pipe-like outcrop is reported
775 and three rock samples (two being from in-situ bodies) have compositions evidencing low
776 crustal contamination and a strong similarity with diamond-producing kimberlites from
777 Gribb, Russian Federation and Diavik, Canada (Hutchison, 2022).

778

779 **Volume potential**

780

781 The presence of diamonds in Greenland is well-established. Of the 3029 diamond-prospective
782 rocks known from Greenland (Hutchison, 2020a), 41 have been proven to be diamond
783 bearing. However, the proportion of Greenlandic indicator mineral samples that were
784 analysed for diamond specifically is low compared to other localities (11% compared to, for
785 example, 84% in Western Australia, Hutchison 2018b). So, considering few known bodies or
786 even discrete occurrences have been tested, the abundance of diamondiferous rocks is
787 significant. Diamonds on occasion are demonstrably large, and occur in commercially-
788 interesting concentrations (Hutchison and Frei, 2009) and mineral chemistry and the results of
789 this study demonstrate significant potential for further discoveries. However, one of the most
790 significant challenges to the commercial significance of Greenland's diamondiferous bodies is
791 volume potential. The sizes of diamond-prospective rocks in Greenland vary considerably,
792 with 5 km being the longest known (the Paternoster Dyke, potentially up to 0.1 km² exposed
793 at surface, Hutchison, 2022) and Garnet Lake is of comparable size to Snap Lake in Canada
794 (Hutchison and Frei, 2009). However, due to glacial weathering, and while this provides
795 opportunities for re-worked deposits (both on and off-shore), most known diamondiferous
796 bodies represent the hypabyssal components of the intrusive plumbing system. That said,
797 bodies not yet known to be diamondiferous, but still diamond-prospective are known from a
798 wider geographic area extending into eastern Greenland at Skjoldungen (Hutchison, 2022a)
799 and include the ultramafic lamprophyre diatremes of southern Greenland (Upton et al., 2006).

800

801

802 **Concluding remarks**

803

804 The Garnet Lake aillikite / kimberlite multiply-intruded dyke system distinguishes itself as a
805 diamondiferous body of commercially interesting volume, diamond size, quality and
806 concentration. Diamonds of 2.39 and 2.51 carats have been recovered from small bulk
807 samples. To the north, within Disko Bay, diamondiferous ultramafic lamprophyres host
808 diamonds with high levels of preservation and colourless diamonds are abundant throughout
809 Greenland. The common presence of dykes and sills, evidencing removal of volcanic
810 components of diamond-hosting rocks infers high quantities of diamonds in sedimentary
811 deposits. Nonetheless, the presence of diatremes of Gardar-age ultramafic lamprophyres also
812 demonstrates the potential for discovery of further bodies with significant volume potential.
813 The mantle lithosphere is demonstrably thick, under a high proportion of Greenland's ice-free
814 coastline, as testified by the presence of diamonds and the chemistries of their companion
815 mantle-derived minerals. Greenland is established as a diamond prospective country.

816 Historical data and regional prospectivity metrics identify further opportunities for
817 diamond exploration in Greenland particularly in selected areas of the west and southern
818 coasts, as well as within less-explored areas such as eastern and northern regions, and off-
819 shore. The NAC of western Greenland, distinguishes itself by numerous known in-situ
820 diamondiferous bodies including the most diamondiferous occurrence in Greenland at Garnet
821 Lake. The northern part of the NAC in western Greenland sits above the thickest (>225 km)
822 mantle lithospheric keel. The Rae Craton of western Greenland contains diamondiferous
823 bodies (as observed in the Rae craton in Canada) and presents a varied range of sampled
824 mantle lithosphere depths and compositions in its regional indicator minerals. It is notable for
825 larger bodies, such as the Paternoster Dyke. The southern Greenland Ketilidian Orogen, and
826 associated Gardar Province, while less geologically stable than the attractive cratonic nuclei
827 hosts prospective mineral chemistries and in-situ ultramafic lamprophyres revealing
828 significant volume potential for exploitation. Further prospective areas that are considerably

829 under-explored for diamonds include the Inglefield Orogenic Belt, NAC and Rae Cratons of
830 eastern Greenland, and the Rae Craton of North Greenland.

831 This work demonstrates that Greenland is considerably under-explored for diamonds
832 and presents compelling geological arguments for further study.

833

834 **Acknowledgements** The author's thirty-one year span of engagement with the geology of
835 Greenland, particularly in the field of diamonds, has been greatly assisted by the
836 companionship and insights of Stefan Bernstein, Lotte Larsen and Troels Nielsen (GEUS),
837 Urban Burger (De Beers Marine), Rory Changleng (Pennsylvania State University), Ole
838 Christiansen (Kommune Kujalleq), Guy Della Valle (independent), John Ferguson
839 (deceased), Chuck Fipke (CF Minerals), Karen Hanghøj (British Geological Survey), Julie
840 Hollis (EuroGeoSurveys), Anette Juul-Nielsen (Government of Greenland), Matilde Rink
841 Jørgensen (Gribskov Gymnasium), Ekaterina Kiseeva (American Museum of Natural
842 History), Louise Nielsen, Graham Pearson (University of Alberta), Geoff Nowell (University
843 of Durham), Jonas Petersen (Government of Greenland), Jennifer Porter, Karina Sand
844 (University of Copenhagen), Agnete Steinfeldt (deceased), Jamie Tuer (Fjordland
845 Exploration), Chad Ulansky (Metalex Ventures) and Brian Upton (University of Edinburgh).
846 They are all gratefully acknowledged. Tjerk Heijboer and Kristine Thrane (GEUS) are
847 thanked for support on classifications and ages of Greenland's geological regions. Barrett
848 Elliott (NTGS) is thanked for contributions regarding Canadian data. Wayne Taylor, Lynton
849 Jaques and Zachary Sudholz are thanked for invaluable insights into mineral chemistry and
850 assisting with geothermobarometric calculations. Thomas Stachel is thanked for provision of
851 PTEXL software. This work was funded by the Government of Greenland. This manuscript
852 benefitted from insightful and constructive reviews by Graham Pearson and Kristoffer Szilas,
853 who are gratefully acknowledged.

854

855

856 **Declarations**

857

858 *Generated by the SNAPP editorial system*

859

860

861 **References**

862

863 Andersen T (1997) Age and petrogenesis of the Qassiarsuk carbonatite-alkaline silicate

864 volcanic complex in the Gardar rift, South Greenland. *Mineral Mag* 61:499–513

865 Artemieva IM (2019) Lithosphere thermal thickness and geothermal heat flux in Greenland

866 from a new thermal isostasy method. *Earth Sci Rev* 188:469–481

867 Banas A, Milne SEM, Stachel T, Stern RA, Pearson DG, Read GH (2025) Diamonds from

868 Fort à la Corne – post-Archean formation in 1 exceptionally cool and fertile lherzolitic

869 substrates. This volume

870 Beard CD, Finch AA, Borst AM, Goodenough KM, Hutchison W, Millar IL, Andersen T,

871 Williams HM, Weller OM (2024) A phlogopite-bearing lithospheric mantle source for

872 Europe's largest REE-HFSE belt: Gardar Rift, SW Greenland. *Earth Planet Sci Lett*

873 640:118780. <https://doi.org/10.1016/j.epsl.2024.118780>

874 Bernstein S, Szilas K, Kelemen PB (2013) Highly depleted cratonic mantle in West

875 Greenland extending into diamond stability field in the Proterozoic. *Lithos* 168–

876 169:160–172

877 Bernstein S, Kokfelt T, Rosa D, Keulen N, Juul-Nielsen A, Keiding JK, Azad NH (2025) Re-

878 assessment of diamond potential for South Greenland. *Geol Surv Denmark Greenland*

879 Rep 2024/35, 30 pp

- 880 Bizzarro M, Simonetti A, Stevenson RK, David J (2002) Hf isotope evidence for a hidden
881 mantle reservoir. *Geology* 30:771–774
- 882 Blichert-Toft J, Rosing MT, Leshner CE, Chauvel C (1995) Geochemical constraints on the
883 origin of the late Archean Skjoldungen alkaline igneous province, SE Greenland. *J*
884 *Petrol* 36/2:515–561
- 885 Bonow J, Lidmar-Bergström K, Japsen, P (2006) Palaeosurfaces in central West Greenland as
886 reference for identification of tectonic movements and estimation of erosion. *Glob*
887 *Planet Change* 50:161–183
- 888 Carlson RW, Irving AJ, Schulze D, Carter Hearn Jr B (2004) Timing of Precambrian melt
889 depletion and Phanerozoic refertilization events in the lithospheric mantle of the
890 Wyoming Craton and adjacent Central Plains Orogen. *Lithos* 77:453–472
- 891 Chapman J, Boxer G (2004) Size distribution analyses for estimating diamond grade and
892 value. *Lithos* 76:369–375
- 893 Day HW (2012) A revised diamond-graphite transition curve. *Amer Mineral* 97:52–62
- 894 Escher JC, Pulvertaft TCR (1995) Geological map of Greenland, 1:2 500 000. *Geol Surv*
895 *Greenland / GEUS Dataverse*. <https://doi.org/10.22008/FK2/SYAL4J>
- 896 Gardiner NJ, Kirkland CL, Hollis JA, Cawood PA, Nebel O, Szilas K, Yakymchuk C (2020)
897 North Atlantic Craton architecture revealed by kimberlite-hosted crustal zircons. *Earth*
898 *Planet Sci Lett* 534:116091, 8 pp. <https://doi.org/10.1016/j.epsl.2020.116091>
- 899 Ghisler M (1990) Geographical subdivisions of Greenland. *Rapport Grønlands Geologiske*
900 *Undersøgelse* 148:8–10
- 901 Griffin WL, Ryan CG (1995) Trace elements in indicator minerals: area selection and target
902 evaluation in diamond exploration. *J Geoch Expl* 53:311–337
- 903 Grütter HS (2009) Pyroxene xenocryst geotherms: techniques and application. *Lithos*
904 112S:1167-1178. <https://doi:10.1016/j.lithos.2009.03.023>

905 Grütter HS, Apter DB (1998) Kimberlite- and lamproite-borne chromite phenocrysts with
906 diamond-inclusion-type chemistries. In: Gurney JJ et al. (eds) Extended Abstracts of
907 the VIIth International Kimberlite Conference. VIIth IKC, pp 280–282

908 Grütter HS, Tuer J (2009) Constraints on deep mantle tenor of Sarfartoq-area kimberlites
909 (Greenland), based on modern thermobarometry of mantle-derived xenocrysts. *Lithos*
910 112S:124–129

911 Grütter HS, Quadling KE (1999) Can sodium in garnet be used to monitor eclogitic diamond
912 potential? In: Gurney JJ, Gurney JL, Pascoe MD, Richardson SH eds. Proc 7th Int
913 Kimberlite Conf, vol 1. Red Roof Design, Cape Town, South Africa, pp 314–320

914 Grütter HS, Gurney JJ, Menzies AH, Winter F (2004) An updated classification scheme for
915 mantle-derived garnet, for use by diamond explorers. *Lithos* 77:841–857

916 Gurney J, Zweistra P (1995) The interpretation of the major element compositions of mantle
917 minerals in diamond exploration. *J Geochem Expl* 53:293–309

918 Haggerty SE (1994) Diamond genesis in a multiply-constrained model. *Nature* 320:34–38

919 Haggerty SE (1999) A Diamond Trilogy: Superplumes, Supercontinents, and Supernovae.
920 *Science* 285:851–860

921 Hasterok D, Chapman DS (2011) Heat production and geotherms for the continental
922 lithosphere. *Earth Planet Sci Lett* 307:59–70

923 Helmstaedt HH, Gurney JJ (1995) Geotectonic controls of primary diamond deposits:
924 implications for area selection. *J Geochem Explor* 53:125–144

925 Henriksen N, Higgins AK, Kalsbeek F, Pulvertaft TCR (2009) Greenland from Archaean to
926 Quaternary. Descriptive text to the 1995 Geological map of Greenland, 1:2 500 000.
927 2nd edition. Geol Surv Denmark Greenland Bull 18, 126 pp and map. Digital map
928 available through www.greenmin.gl

929 Hutchison MT (2012) Diamond exploration of the Northern Territory. Northern Territory
930 Geol Surv Record 2012-001, 64 pp

931 Hutchison MT (2013) Diamond Exploration and Regional Prospectivity of the Northern
932 Territory of Australia. In: Pearson DG et al. (eds) Proceedings of 10th International
933 Kimberlite Conference, vol 2. Spec Issue J Geol Soc India. Geol Soc India, pp 257–
934 280

935 Hutchison MT (2018a) Diamond exploration and regional prospectivity of Western Australia.
936 Mineral Petrol 112S2:737–753

937 Hutchison MT (2018b) Diamond exploration and prospectivity of Western Australia. Geol
938 Surv Western Australia Report 179, 70 pp

939 Hutchison MT (2020a) Greenland diamond exploration data package. Govt Greenland Dept
940 Geol Digital Data Package / GEUS Dataverse. <https://doi.org/10.22008/FK2/VYJX5D>

941 Hutchison MT (2020b) Data methods applied in the Greenland diamond exploration package.
942 Govt Greenland Dept Geol Report 1, 56 pp. GEUS Dataverse.
943 <https://doi.org/10.22008/FK2/RUCP1J>

944 Hutchison MT (2022) Diamond Exploration and Prospectivity of Greenland. Govt Greenland
945 Dept Geol Record 1, 228 pp. GEUS Dataverse.
946 <https://doi.org/10.22008/FK2/HMLDVH>

947 Hutchison MT, Frei D (2009) Kimberlite and related rocks from Garnet Lake, West
948 Greenland, including their mantle constituents, diamond occurrence, age and
949 provenance. Lithos 112:318–333

950 Hutchison MT, Heaman LM (2008) Chemical and physical characteristics of diamond
951 crystals from Garnet Lake, Sarfartoq, West Greenland: an association with carbonatitic
952 magmatism. Canad Mineral 46:1063–1078

953 Hutchison MT, Faithfull JW, Barfod D, Hughes JW, Upton BJ (2018) The mantle of Scotland
954 viewed through the Glen Gollaidh aillikite. Mineral Petrol 112S1:S115–S132

- 955 Hutchison MT, Kirkland CK, Ribeiro B, Bernstein S (2024) Geochronology of the Qeqertaa
956 Diamondiferous Ultramafic Lamprophyre, West Greenland. *J Int Kimberlite Conf*
957 *Abstr* 12, 3 pp. <https://doi.org/10.29173/ikc4034>
- 958 Jensen SM, Secher K, Rasmussen TM, Schjøth F (2004) Diamond exploration data from West
959 Greenland: 2004 update and revision. *Geol Surv Denmark Greenland Rep*, vol
960 2004/117, 90 pp and DVD data package
- 961 Larsen LM, Rex DC (1992) A review of the 2500 Ma span of alkaline-ultramafic, potassic
962 and carbonatitic magmatism in West Greenland. *Lithos* 28:367–402
- 963 Larsen LM, Rønsbo J (1993) Conditions of origin of kimberlites in West Greenland: new
964 evidence from the Sarfartoq and Sukkertoppen regions. *Rapport Grønlands Geologiske*
965 *Undersøgelse* 159:115–120
- 966 Larsen LM, Heaman LM, Creaser RA, Duncan RA, Frei R, Hutchison M (2009)
967 Tectonomagmatic events during stretching and basin formation in the Labrador Sea
968 and the Davis Strait: evidence from age and composition of Mesozoic to Paleogene
969 dyke swarms in West Greenland. *J Geol Soc, London* 166:999–1012
- 970 Lee DC, Milledge HJ, Reddcliffe TH, Scott Smith BH, Taylor WR, Ward LM (1997) The
971 Merlin kimberlites, Northern Territory, Australia. *Russ Geol Geophys* 38:82–96
- 972 McMartin I, McClenaghan MB (2001) Till geochemistry and sampling techniques in
973 glaciated shield terrain: a review. In: McClenaghan MB, Bobrowsky PT, Hall GEM,
974 Cook SJ (eds) *Drift exploration in glaciated terrain*. *Geol Soc Spec Publ* 185, pp 19–83
- 975 Mitchell, RH (1986) *Kimberlites mineralogy, geochemistry and petrology*. Plenum Press,
976 New York, 441 pp
- 977 Moss S, Porritt L, Pollock K, Fomradas G, Stublely M, Eichenberg D, Cutts J (2018) *Geology,*
978 *mineral chemistry and structure of the kimberlites at Diavik Diamond Mine: Indicators*
979 *of cluster-scale cross-fertilisation, mantle provenance and pipe morphology*. *Soc*
980 *Econom Geol Spec Pub* 20:287–318

981 Nielsen TF, Jensen SM (2005) The Majuagaa calcite-kimberlite dyke, Maniitsoq, southern
982 West Greenland. Geol Surv Denmark Greenland Rep 2005/43, 59 pp

983 Nimis P, Taylor WR (2000) Single clinopyroxene thermobarometry for garnet peridotites.
984 Part I. Calibration and testing of a Cr-in-Cpx barometer and an enstatite-in-Cpx
985 thermometer. Contrib Miner Petrol 139(5):541–554

986 Northwest Territories Geological Survey KIDD/KIMC (2017) The Northwest Territories
987 Geological Survey Kimberlite Indicator and Diamond (KIDD) and Kimberlite
988 Indicator Mineral Chemistry (KIMC) databases. Northwest Territories Geological
989 Survey, Canada. Accessed 6th February 2022 at <https://app.nwtgeoscience.ca/>

990 Nutman A, Bennett VC, Hidaka H, Henriksen N, Ali S (2019) The Archean Victoria Fjord
991 terrane of northernmost Greenland and geodynamic interpretation of Precambrian
992 crust in and surrounding the Arctic Ocean. J Geodyn 129:3–23

993 Pearson DG, Scott JM, Liu J, Schaeffer A, Wang LH, van Hunen J, Szilas K, Chacko T,
994 Kelemen PB (2021) Deep Continental Roots and Cratons. Nature 596:199–211.
995 <https://doi.org/10.1038/s41586-021-03600-5>

996 Pell J, Neilson S (2008) Assessment Report on the Chidliak Property, 66° 21' 43" W, 64°28'
997 26" N Baffin Region, Nunavut. License Report for Peregrine Diamonds Ltd., Arch
998 Nunavut Geosc Report File, vol 85402, 127 pp, 13 appendices, 9 maps

999 Pell J, Neilson S (2012) Assessment Report on till sampling & geochemistry, airborne
1000 geophysics, ground geophysical surveys and diamond drilling on the Chidliak Project
1001 in 2010 & 2011, 66° 21' 43" W, 64°28' 26" N Baffin Region, Nunavut. License
1002 Report for Peregrine Diamonds Ltd., Arch Nunavut Geosc Report File, vol 85721, 425
1003 pp, 18 appendices

1004 Ramsay RR (1992) Geochemistry of diamond indicator minerals. PhD thesis, Department of
1005 Geology and Geophysics, University of Western Australia (unpublished report)

- 1006 Ramsay RR, Tompkins LA (1994) The geology, heavy mineral concentrate mineralogy, and
1007 diamond prospectivity of the Boa Esperança and Cana Verde Pipes, Corrego D'Anta,
1008 Minas Gerais, Brazil. *Companhia de Pesquisa de Recursos Minerais – CPRM Spec*
1009 *Publ 1B Jan/94:329–345*
- 1010 Robles-Cruz S, Watangua M, Isidoro L, Melgarejo J (2008) Contrasting compositions and
1011 textures of ilmenite in the Catoca kimberlite, Angola, and implications in exploration
1012 for diamond. *Lithos 112S:966–975*
- 1013 Sand KK, Waight TE, Pearson DG, Nielsen TRD, Makovicky E, Hutchison MT (2009) The
1014 lithospheric mantle below southern West Greenland: a geothermobarometric approach
1015 to diamond potential and mantle stratigraphy. *Lithos 112S:1155–1166*
- 1016 Secher K, Heaman LM, Nielsen TFD, Jensen SM, Schjøth F, Creaser RA (2009) Timing of
1017 kimberlite, carbonatite, and ultramafic lamprophyre emplacement in the alkaline
1018 province located 64°–67° N in southern West Greenland. *Lithos, 112S:400–406*
- 1019 Stachel T, Banas A, Aulbach S, Smit KV, Wescott P, Chinn I, Fisher D, Kong J (2017) The
1020 Victor Diamond Mine (Superior Craton, Canada) – A new paradigm for exploration in
1021 unconventional settings. *J Int Kimberlite Conf Abs. 11:11IKC-4453, 3 pp*
- 1022 Sudholz ZJ, Yaxley GM, Jaques AL, Brey GP (2021a) Experimental recalibration of the
1023 Cr-in-clinopyroxene geobarometer: improved precision and reliability above 4.5 Gpa.
1024 *Cont Mineral Petrol 176:11, 20 pp. <https://doi.org/10.1007/s00410-020-01768-z>*
- 1025 Sudholz ZJ, Yaxley GM, Jaques AL, Chen J (2021b) Ni-in-garnet geothermometry in mantle
1026 rocks: a high pressure experimental recalibration between 1100 and 1325 °C. *Cont*
1027 *Mineral Petrol 176:32, 16p. <https://doi.org/10.1007/s00410-021-01791-8>*
- 1028 Upton BGJ, Emeleus CH, Heaman LM, Goodenough KM, Finch AA (2003) Magmatism of
1029 the mid-Proterozoic Gardar Province, South Greenland: chronology, petrogenesis and
1030 geological setting. *Lithos 68:43–65*

1031 Upton BGJ, Craven, JA, Kirstein LA (2006) Crystallisation of mela-aillikites of the Narsaq
1032 region, Gardar alkaline province, south Greenland and relationships to other aillikitic–
1033 carbonatitic associations in the province. *Lithos* 92:300–319

1034 van Hinsberg V, Crotty C, Roozen S, Szilas K, Kisters A (2018) Pressure–Temperature
1035 History of the >3 Ga Tartoq Greenstone Belt in Southwest Greenland and Its
1036 Implications for Archaean Tectonics. *Geosci* 8:367.
1037 <https://doi:10.3390/geosciences8100367>

1038 Weidick A, Bennike O (2006) Quaternary glaciation history and glaciology of Jakobshavn
1039 Isbræ and the Disko Bugt region, West Greenland: a review. *Geol Surv Denmark*
1040 *Greenland Bull* 14, 78 pp

1041 Wittig N, Webb M, Pearson DG, Dale CW, Ottley CJ, Hutchison M, Jensen SM, Luguet A
1042 (2010) Formation of the North Atlantic Craton: Timing and mechanisms constrained
1043 from Re–Os isotope and PGE data of peridotite xenoliths from S.W. Greenland. *Chem*
1044 *Geol* 276:166–187

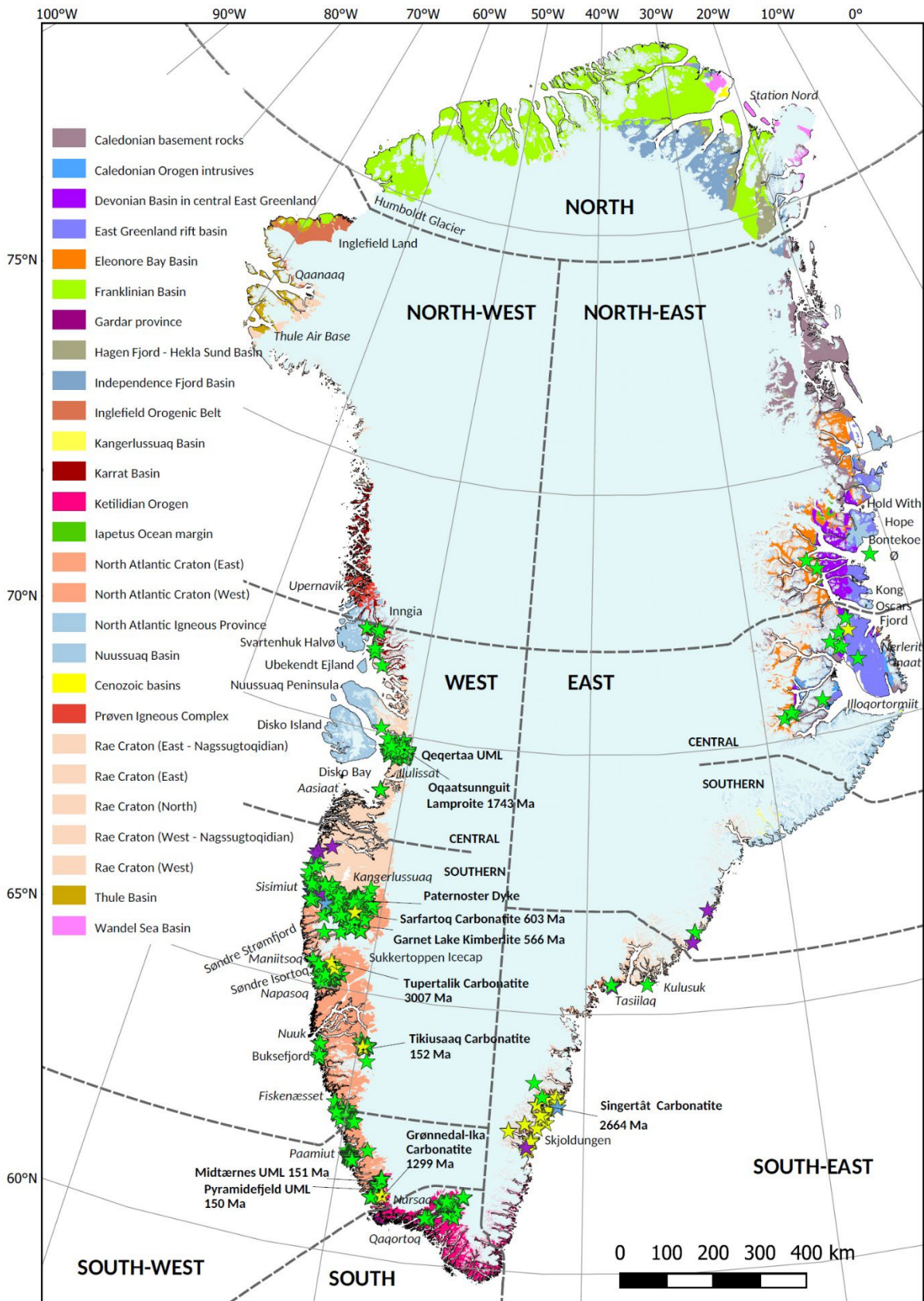
1045 Wyatt BA, Baumgartner M, Anckar E and Grütter H (2004) Compositional classification of
1046 "kimberlitic" and "nonkimberlitic" ilmenite: *Lithos* 77:819–840

1047 Ziberna L, Nimis P, Kuzmin D, Malkovets VG (2016) Error sources in single-clinopyroxene
1048 thermobarometry and a mantle geotherm for the Novinka kimberlite, Yakutia. *Am*
1049 *Mineral* 101(10):2222–2232

1050

1051 **Figures**

1052



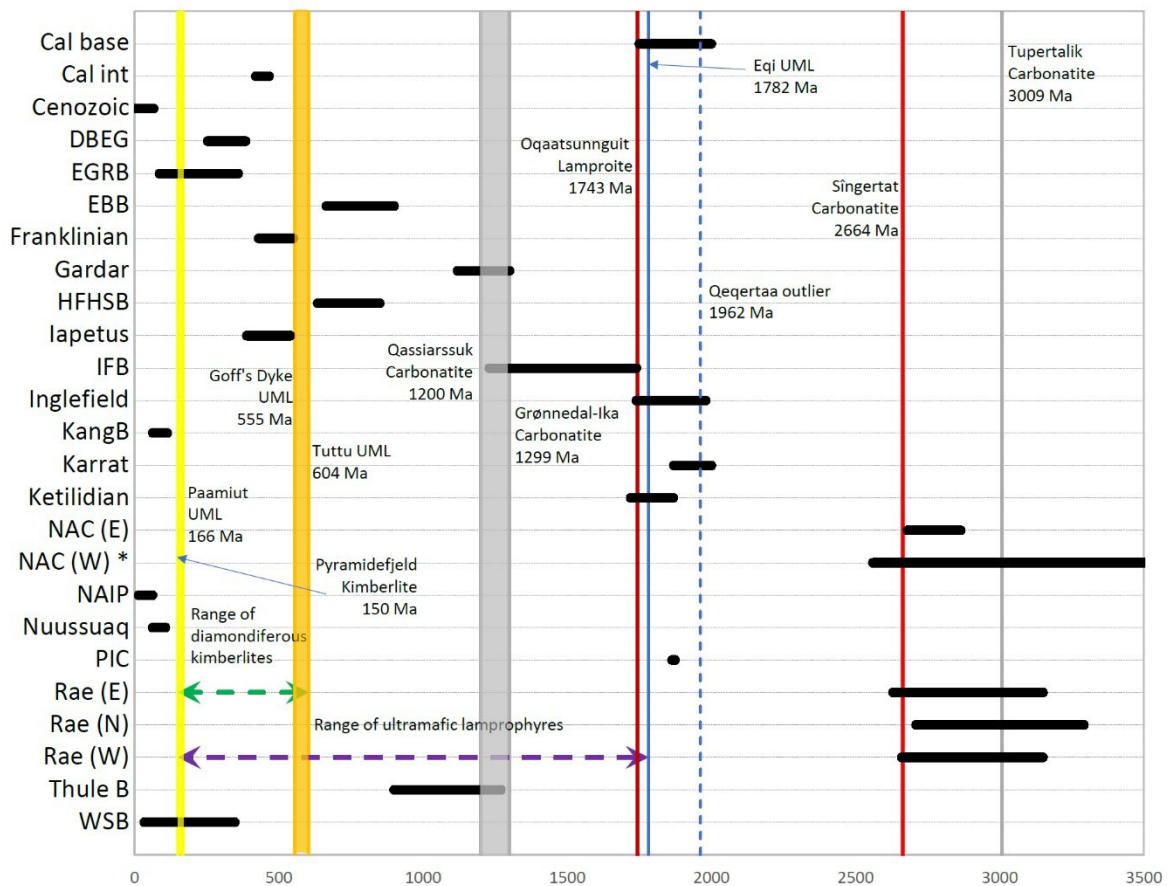
1053

1054

1055 **Fig. 1** Geographic and geological locations of note for diamond exploration in Greenland.

1056 Geographic subdivisions follow Ghisler (1990) and are applied throughout the text.

1057 Geological regions are modified from Escher and Pulvertaft (1995) as described in the text
1058 and form the basis for diamond prospectivity modelling. Principal placenames referenced in
1059 the text are included. In-situ occurrences of known kimberlites and ultramafic lamprophyres,
1060 including aillikites (green stars), lamproites (purple stars), carbonatites (yellow stars), and
1061 their coarse-grained variety, sövites (blue stars), are indicated with principal sites named.
1062 Favoured emplacement ages, following Hutchison (2020a), are indicated for selected bodies.
1063 Figure modified from Hutchison (2022)

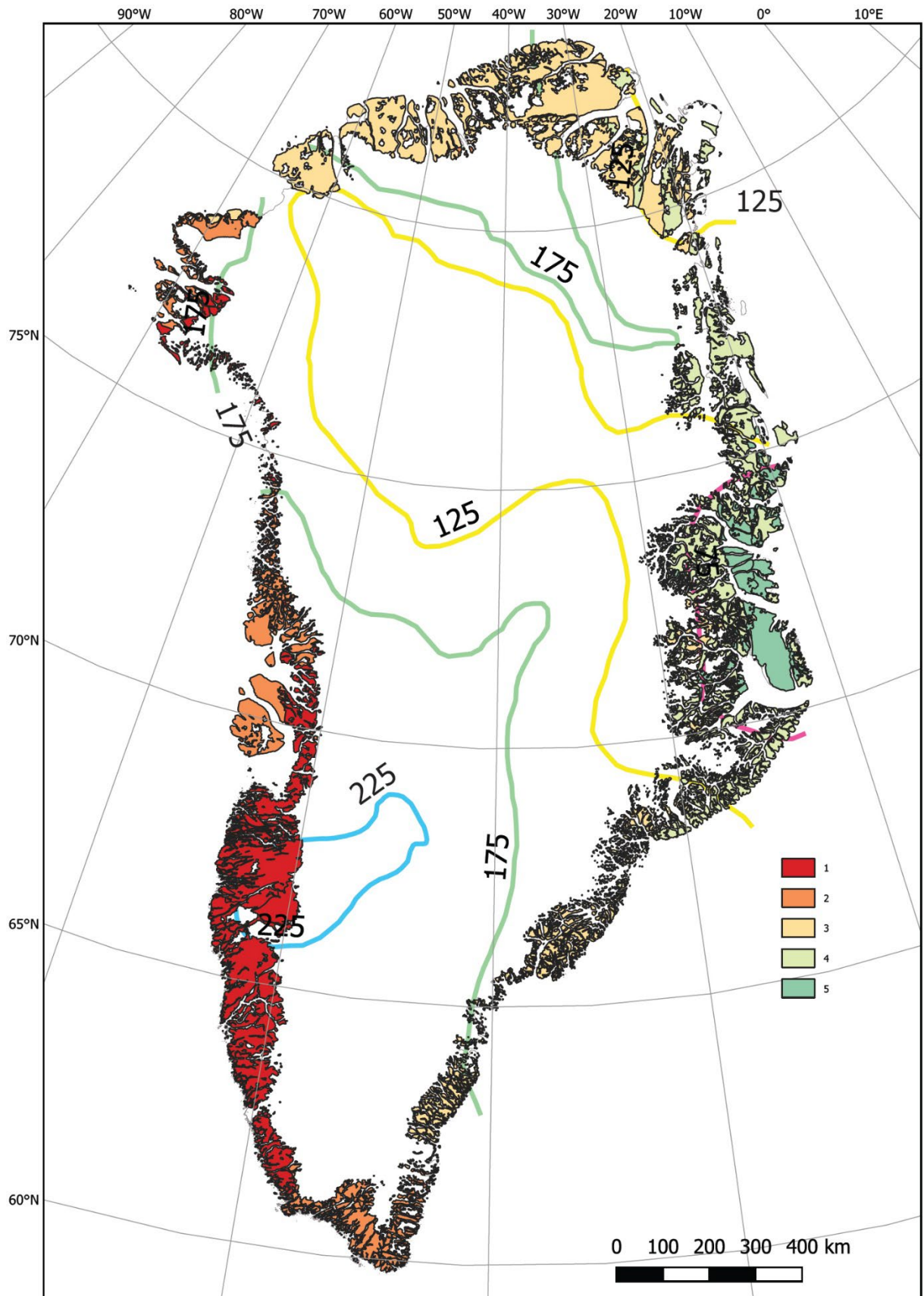


1064

1065

1066 **Fig. 2** Ranges of ages (Ma) of rocks present in geological regions of Greenland in the context
 1067 of ages of selected diamond-prospective rocks. References to age ranges in Henriksen et al.
 1068 (2009) and Hutchison (2022). Cal base = Caledonian Orogen basement, Cal int = Caledonian
 1069 Orogen intrusives, Cenozoic = Cenozoic basins, DBEG = Devonian Basin of East Greenland,
 1070 EGRB = East Greenland Rift Basin, EBB = Eleanore Bay Basin, Franklinian = Franklinian
 1071 Basin, Gardar = Gardar Province, HFHSB = Hagen Fjord - Hekla Sund Basin, Iapetus =
 1072 Iapetus Ocean Margin, IFB = Independence Fjord Basin, Inglefield = Inglefield Orogenic
 1073 Belt, KangB = Kangerlussuaq Basin, Karrat = Karrat Basin, Ketilidian = Ketilidian Orogen,
 1074 NAIP = North Atlantic Igneous Province, Nuussuaq = Nuussuaq Basin, PIC = Prøven Igneous
 1075 Complex, Rae (E), (N) and (W) = Rae Craton of eastern, northern and western Greenland
 1076 respectively, Thule B = Thule Basin, WSB = Wandel Sea Basin. * The NAC of west
 1077 Greenland rocks extend in age to 3890 Ma. The youngest and oldest-dated intrusives for each
 1078 age cluster are indicated. The single outlier of 1962±80 Ma from Th/Pb age determination of

1079 a monazite grain from the diamondiferous Qeqertaa UML is shown, older than the peak
1080 metamorphic ages from two samples at 1788 ± 16 Ma and 1819 ± 23 Ma and possibly
1081 representing an emplacement age (Hutchison et al., 2024). For reference, the diamondiferous,
1082 multiply intruded aillikite / kimberlite at Garnet Lake, Sarfartoq (NAC of western Greenland)
1083 has been dated at 566 Ma (Hutchison and Heaman, 2008) and lies at the later end of the
1084 Neoproterozoic (Ediacaran) western Greenlandic kimberlitic cluster



1085

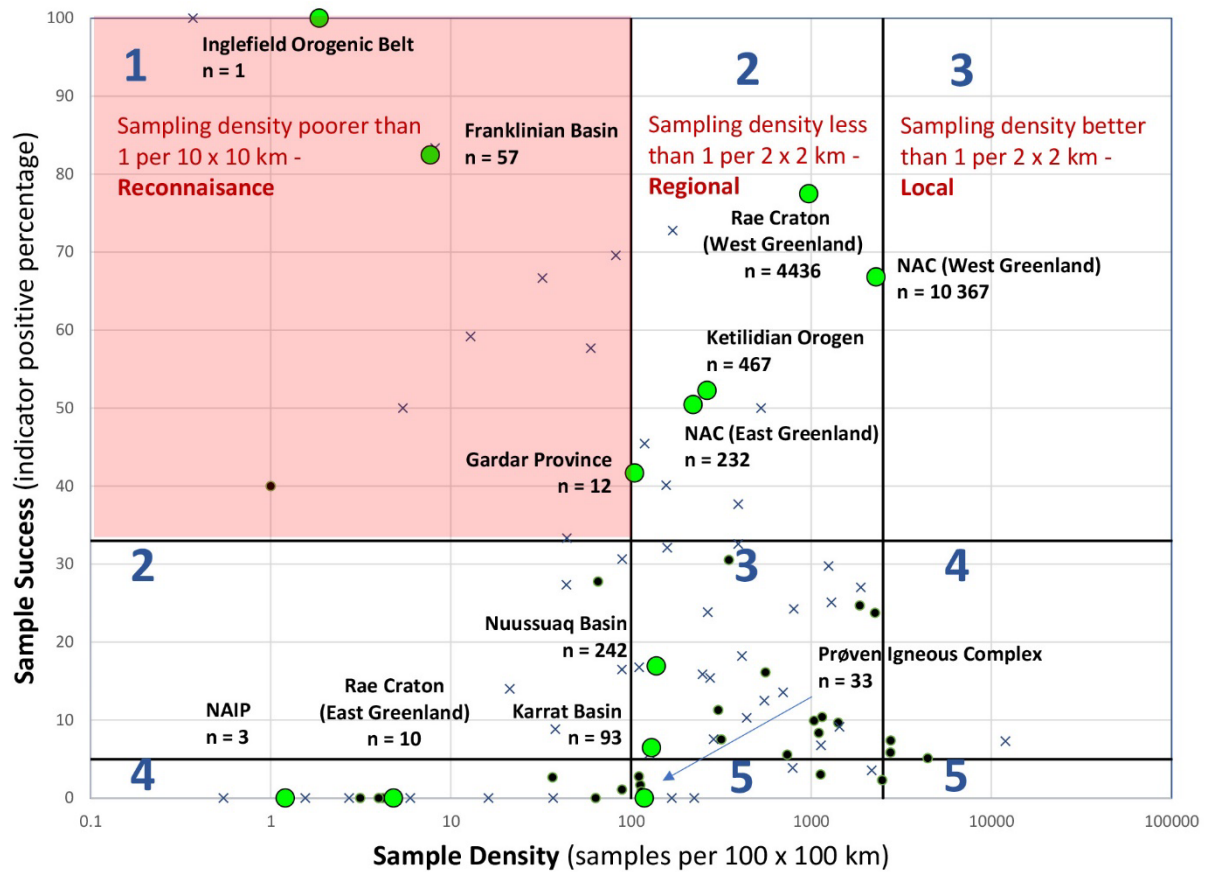
1086

1087

1088

Fig. 3 Geological regions scored according to lithosphere thickness. The surface area above each range of depths to the asthenosphere / lithosphere boundary (shown by the coloured lines

1089 and following Artemieva, 2019) was calculated for each geological region and a weighted
1090 depth calculated. These weighted depths were used to assign a score to each geological region
1091 with lower values representing thicker, and thus more diamond-prospective mantle
1092 lithosphere. While the prominent mantle keel in excess of 250 km in western Greenland
1093 results in a good score for the Rae Craton and NAC in this area, it is notable that Inglefield
1094 Land in northern North-West Greenland scores well. Significant mantle thinning as a
1095 consequence of the Caledonian Orogeny results in poor scores for eastern Greenlandic regions
1096 centred on 72°N (Kong Oscars Fjord)

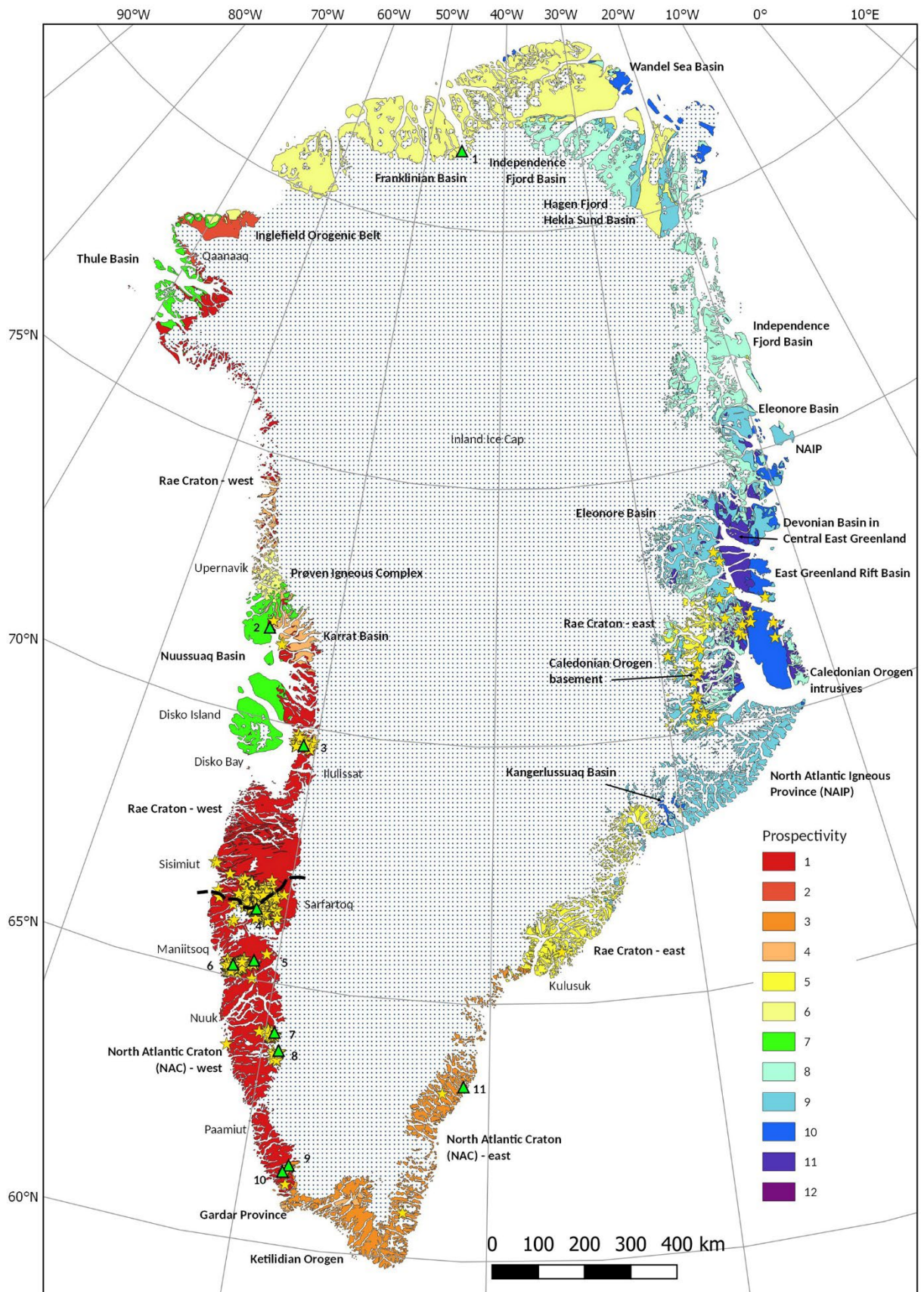


1097

1098

1099 **Fig. 4** Sampling success versus sampling density for samples taken for diamond indicator
 1100 identification. Geological regions are labelled, with the numbers of indicator mineral samples
 1101 shown (both positive and negative samples). Sampling success is measured as the percentage
 1102 of samples collected for diamond indicator minerals that returned a positive recovery (i.e., at
 1103 least one visually determined indicator mineral, including diamond). Sampling density is the
 1104 number of samples (n) taken per 10 000 km² area within each region. Blue numbers represent
 1105 prospectivity scores assigned to regions plotting within shaded areas of the chart. Regions
 1106 with good indicator recovery (over 1/3 of samples being positive) but explored only at
 1107 reconnaissance scale (<math>< 1 \text{ sample per } 100 \text{ km}^2</math>) are favoured. Regions with poor recovery
 1108 (under 1/20 of samples being positive) that have been sampled with average sampling density
 1109 better than 1 sample per 100 km² are less favoured (scoring 5). Completely unsampled areas,
 1110 not represented in the figure, are scored 5 or 6, depending on whether lack of sampling is
 1111 based on geological or logistical reasons. Data from the Northern Territory (Hutchison, 2012,

1112 black dots) and Western Australia (Hutchison, 2018b, crosses) are provided for comparison,
1113 showing that relative to the diamond-producing nation of Australia, Greenland is significantly
1114 under-sampled, whereas the sampling which has occurred has been more directed, and thus
1115 more successful

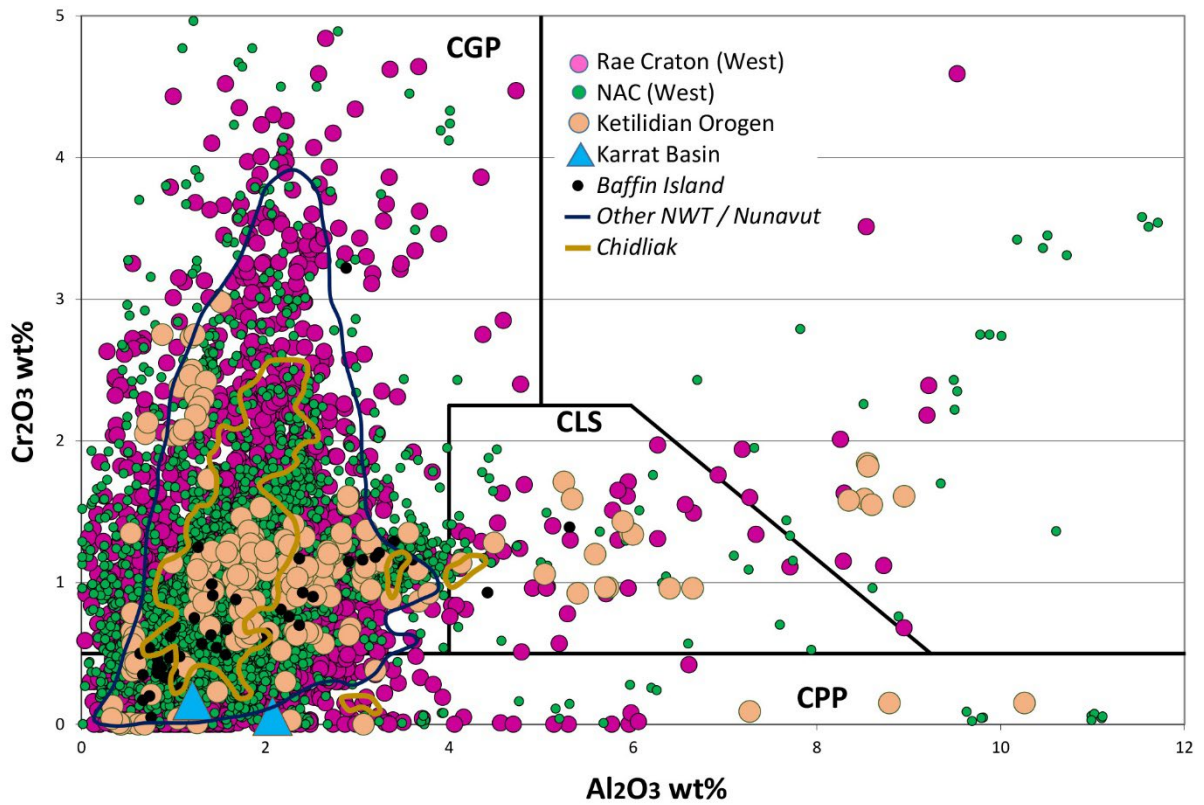


1116

1117

1118 **Fig. 5** Prospectivity map of Greenland. Geological sub-divisions are ranked for prospectivity,
 1119 following the methodology described in the text, in the context of mantle structure, the age of

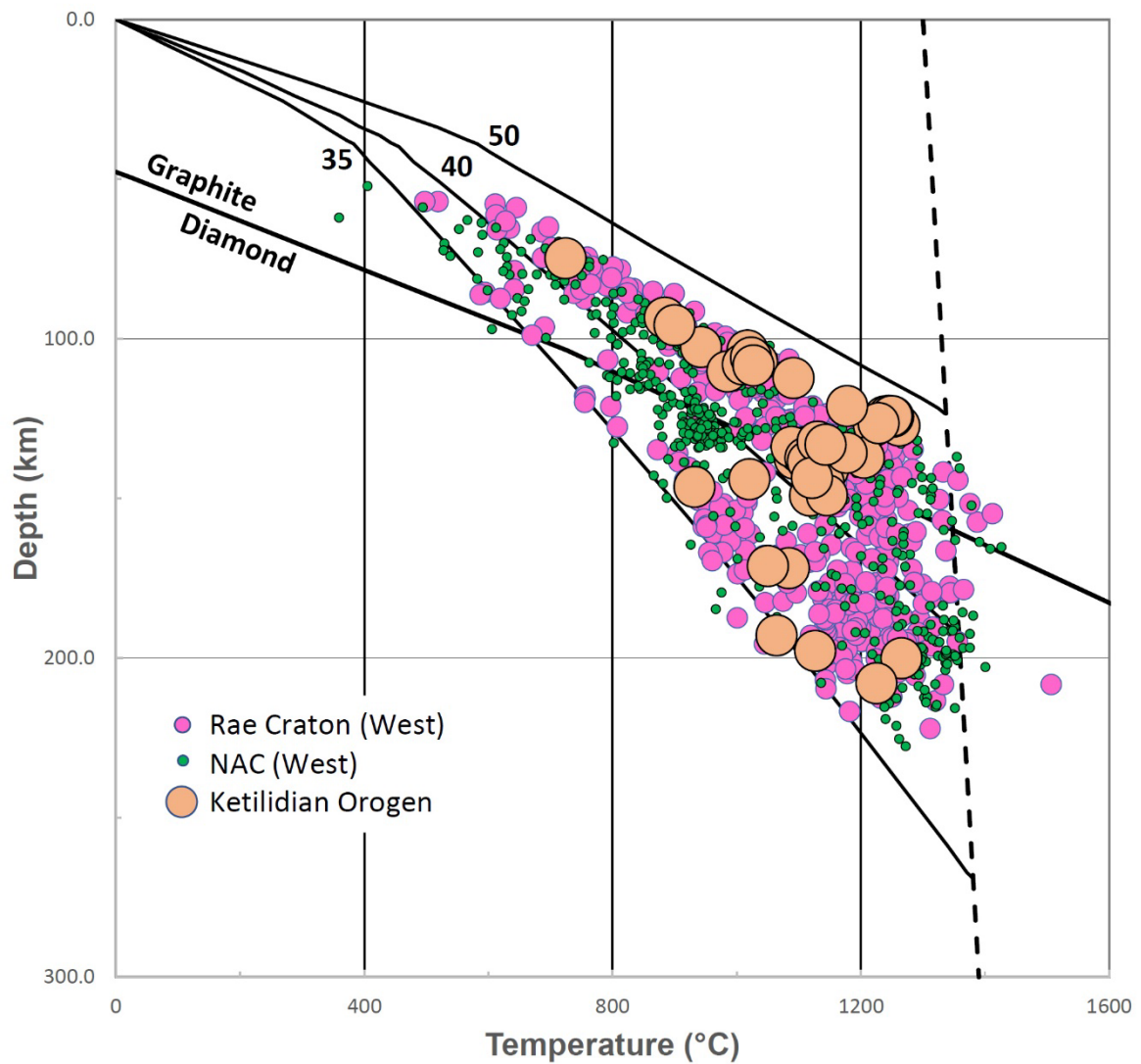
1120 surface rocks, the extent of sample coverage and recovery of visually-determined indicators.
1121 Ranking follows the key, with 1 being the most prospective area and 12 the least. Areas of
1122 permanent ice are identified by stippling. In-situ diamond-prospective rocks are shown by
1123 yellow stars, with notable localities numbered and identified by green triangles: 1 – Rae
1124 Craton of north Greenland with associated visually identified garnets, 2 – Svartenhuk Halvø,
1125 3 – Qeqertaa diamondiferous metamorphosed ultramafic lamprophyre dykes, 4 – Garnet Lake
1126 diamondiferous multiply intruded aillikite / kimberlite sheet, 5 – Qaamasoq diamondiferous
1127 kimberlitic float, 6 – Majuagaa diamondiferous kimberlite dyke, 7 – Tikiusaaq Carbonatite
1128 and associated diamondiferous aillikite dykes, 8 – Nunatak 1390 with abundant kimberlitic
1129 float, 9 – Midternæs diamondiferous aillikite sills, 10 – Pyramidefjeld diamondiferous
1130 aillikite sheets, 11 – Skjoldungen Carbonatite complex and neighbouring indicator garnet and
1131 possible kimberlite



1132

1133

1134 **Fig. 6** Chemical composition of clinopyroxenes in terms of Cr_2O_3 and Al_2O_3 . Compositional
 1135 fields CGP (clinopyroxene from garnet peridotite), CLS (clinopyroxene from spinel
 1136 lherzolite) and CPP (eclogitic, megacrystic and cognate clinopyroxene) are from Ramsay and
 1137 Tompkins (1994). Greenland clinopyroxene compositions are presented following the key.
 1138 For comparison, a hand-drawn field for regional samples from Nunavut and Northwest
 1139 Territories reflects 99% of the compositional data range omitting outliers (Northwest
 1140 Territories Geological Survey, KIDD/KIMC, 2017). Individual compositions from Brodeur
 1141 Peninsula (Rae Craton in Canada) samples are also included, as is an approximated field of
 1142 90% of Chidliak samples reported by Pell and Neilson (2008)

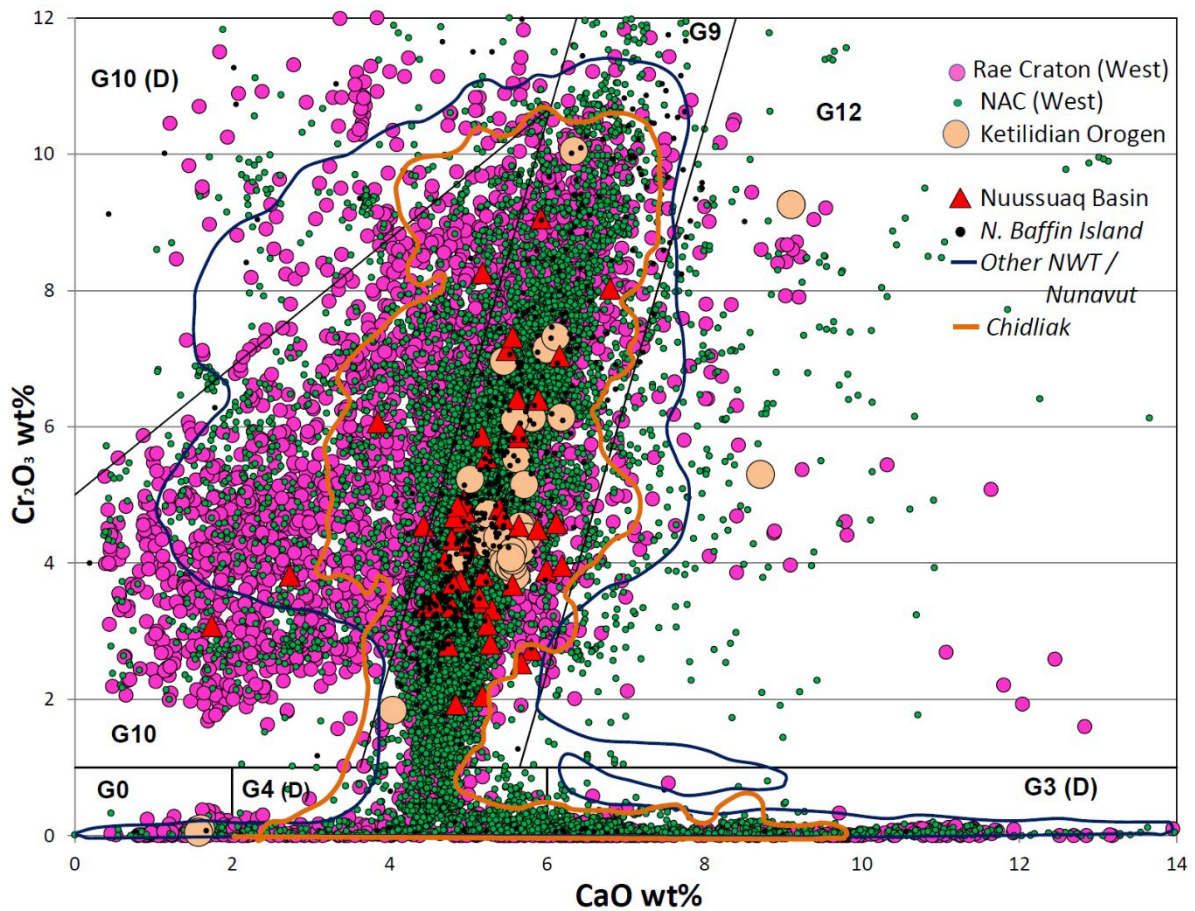


1143

1144

1145 **Fig. 7** Calculated temperature and depths of origin of garnet lherzolite-derived clinopyroxenes
 1146 grains from surface sediment and solid rock samples, following the methodology of Sudholz
 1147 et al. (2021a). The diamond-graphite phase transition of Day (2012) is annotated, and dashed
 1148 mantle adiabat and 35, 40 and 50 mWm⁻² geotherms of Hasterok and Chapman (2011) are
 1149 shown. High proportions of clinopyroxenes derive from within the diamond stability field.
 1150 North Atlantic Craton grains, among which is the deepest calculated clinopyroxene (Garnet
 1151 Lake sample from 228 km, 74.5 kbar, 1272 °C), express a slightly tighter clustering of
 1152 formation conditions than Rae Craton grains. While several Ketilidian Orogen grains express
 1153 a relatively warm ~44 mWm⁻² geotherm, deeper-sourced grains clearly demonstrate a

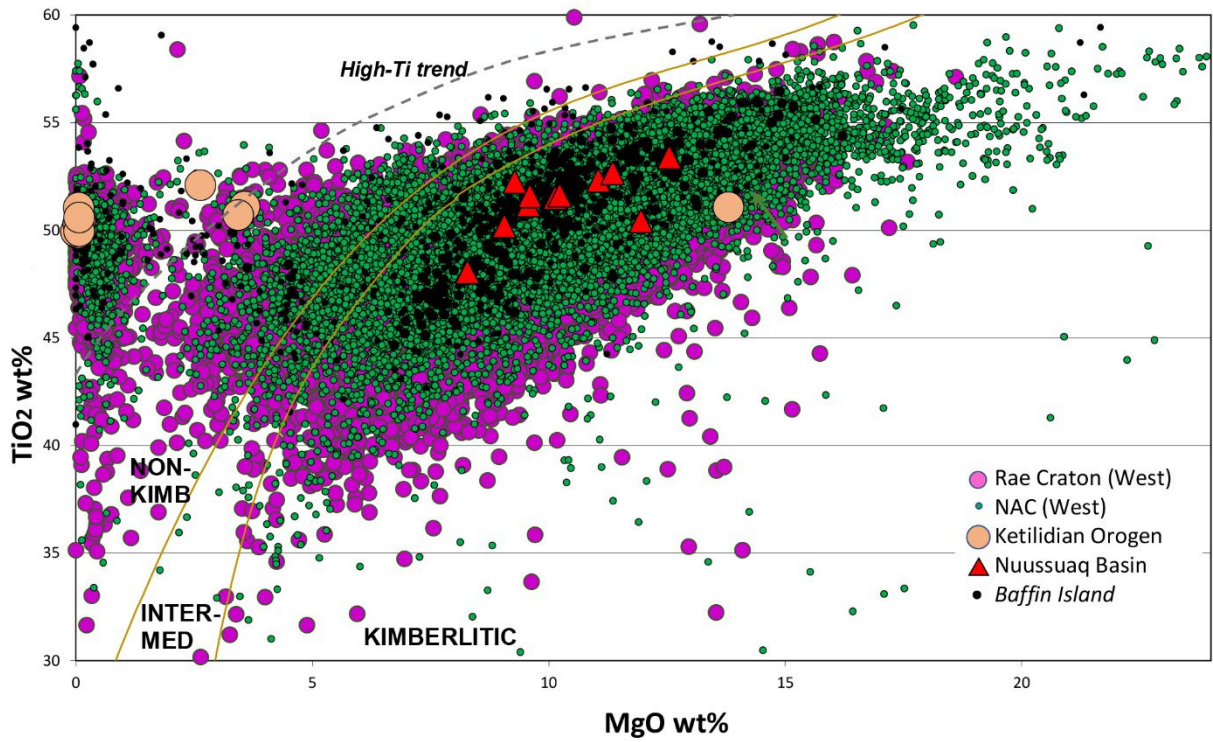
1154 considerably cooler geotherm comparing favourably with deep-sourced clinopyroxenes from
1155 the Rae and North Atlantic Cratons, and particularly conducive to diamond formation



1156

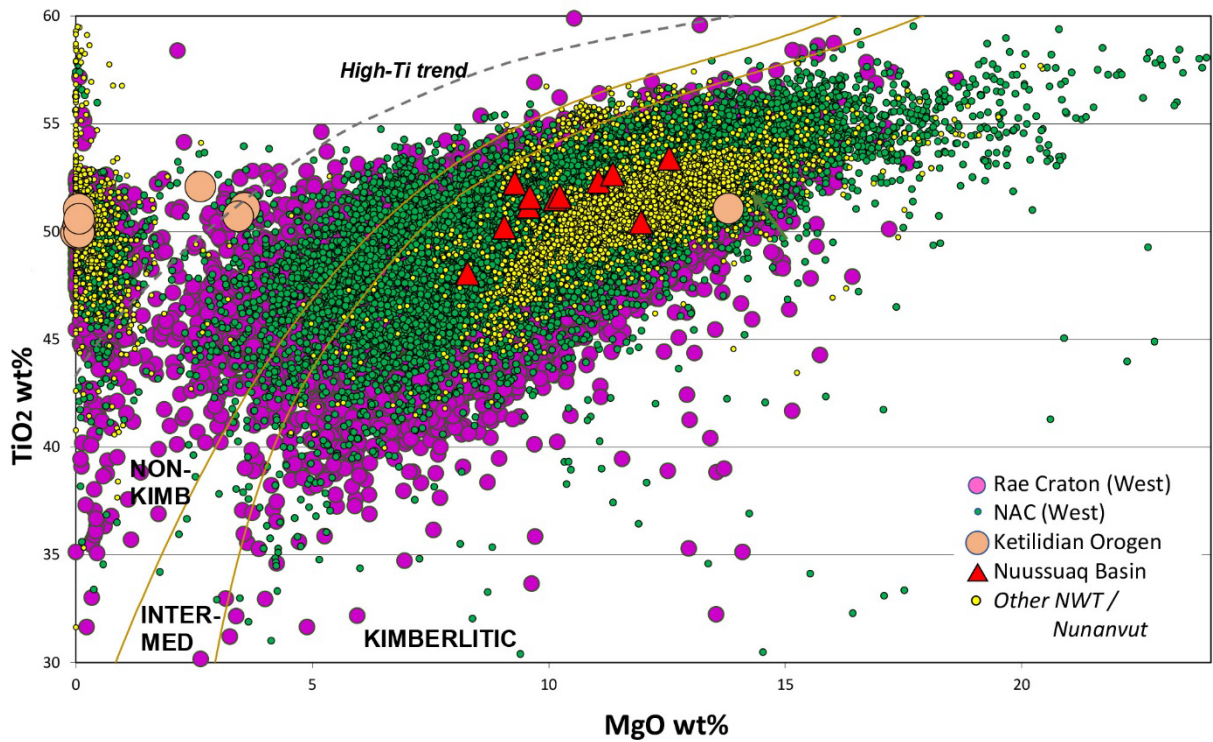
1157

1158 **Fig. 8** Chemical composition of pyrope–almandine–grossular garnets in terms of CaO and
 1159 Cr₂O₃. Classifications follow Grütter and Quadling (1999) and Grütter et al. (2004).
 1160 Compositions of Greenlandic garnets are subdivided according to the key. For comparison,
 1161 the extent of 99% of Nunavut and Northwest Territories compositions from Northwest
 1162 Territories Geological Survey, KIDD/KIMC (2017) indicator garnets is shown, as are
 1163 individual compositions from the Brodeur Peninsula (Rae Craton in Canada) from the same
 1164 reference. The range of approximately 90% of garnet indicator compositions from till samples
 1165 from Chidliak (Pell and Neilson, 2012) is also shown



1166

1167



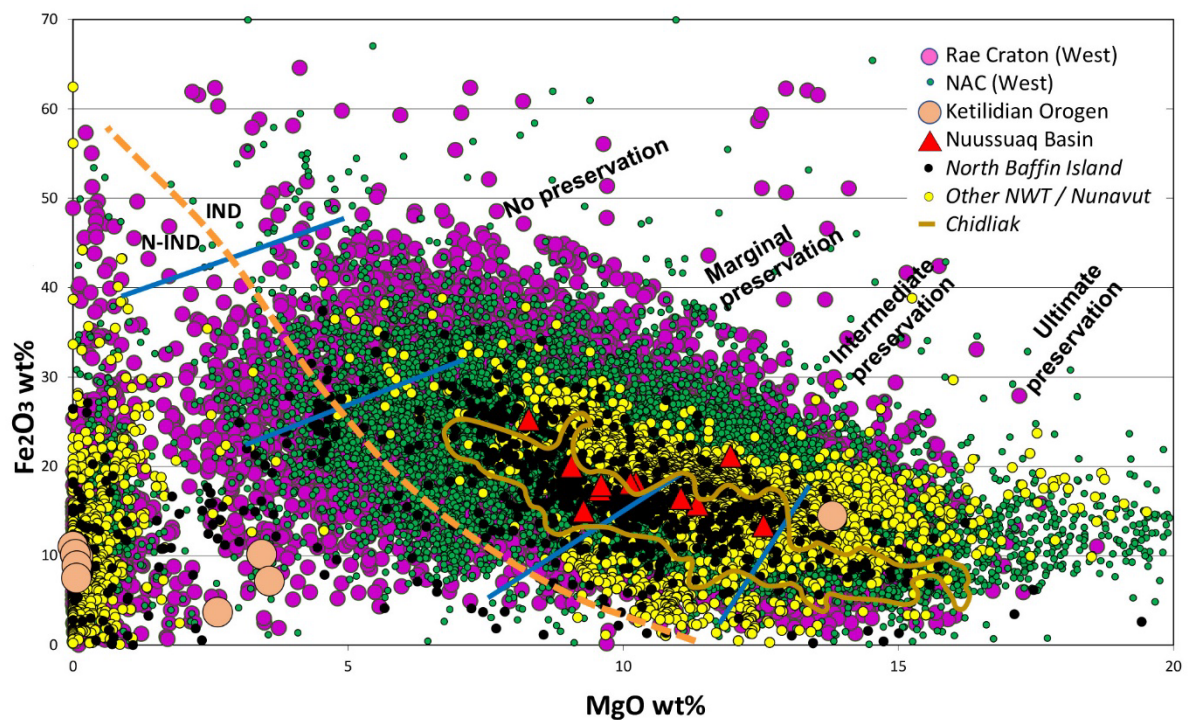
1168

1169

1170 **Fig. 9** Chemical composition of ilmenites in terms of TiO₂ and MgO. Mineral chemistry is
 1171 subdivided according to likely association with kimberlite following Wyatt et al. (2004).

1172 Compositions of Greenlandic ilmenites from different localities are plotted according to the

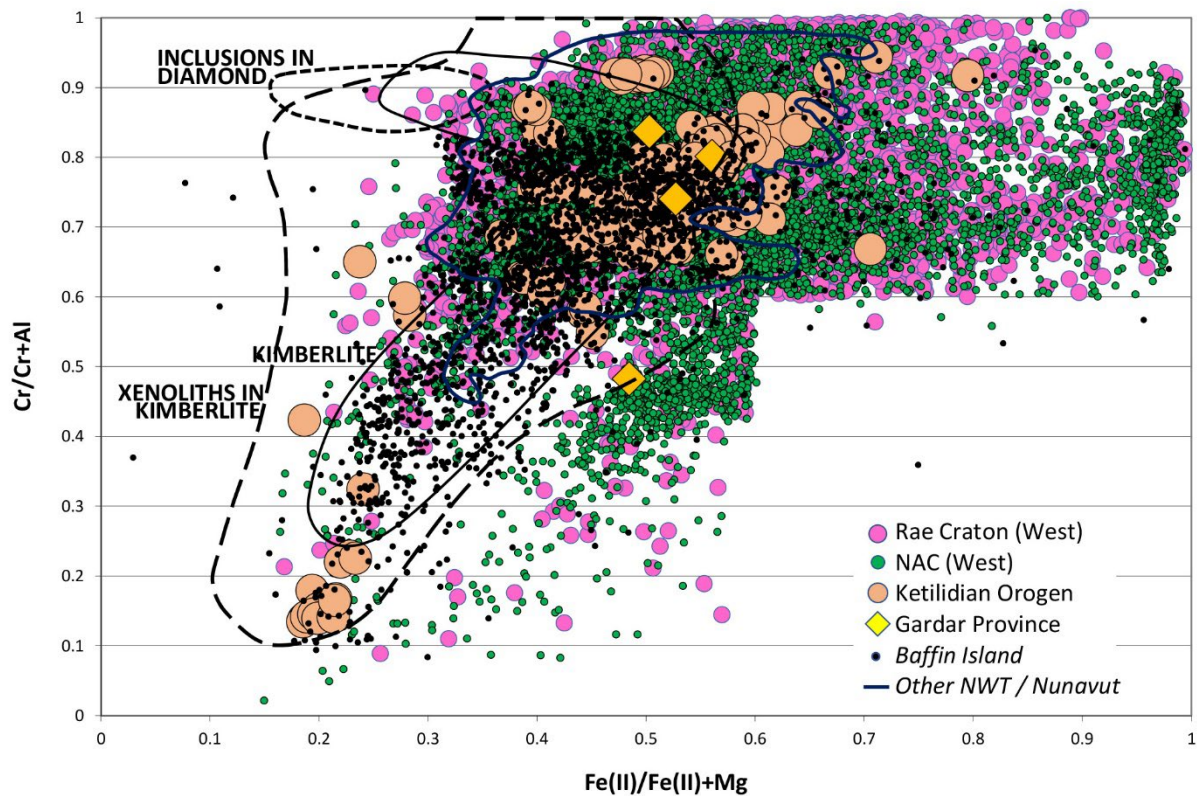
1173 key: a) Greenlandic ilmenite compositions in comparison with Canadian samples from
1174 northern Baffin Island Brodeur Peninsula diamondiferous kimberlite field (Northwest
1175 Territories Geological Survey, KIDD/KIMC, 2017). Both the NAC and Rae Cratons of
1176 western Greenland reveal very abundant numbers of ilmenites well within the field of
1177 compositions associated with kimberlite. All Nuussuaq Orogen ilmenites fall firmly within
1178 the kimberlitic field, and while the numbers of Ketilidian Orogen ilmenites with
1179 compositional data are very small (12 samples), one analysis plots within the kimberlite field.
1180 While NAC ilmenites from western Greenland extend to particularly high Mg-concentrations,
1181 Brodeur Peninsula ilmenite compositions sit comfortably within NAC and Rae Craton
1182 compositional fields and, in particular, are closely mirrored by Nuussuaq Basin samples; b)
1183 Greenlandic ilmenite compositions compared with the range of 99% of Canadian ilmenites
1184 from Northwest Territories Geological Survey, KIDD/KIMC (2017) excluding Brodeur
1185 Peninsula samples



1186

1187

1188 **Fig. 10** Distribution of ilmenite compositions in terms of ferric iron oxide ($\text{Fe(III)}_2\text{O}_3$) and
 1189 MgO wt% for Greenlandic and selected Canadian sources. All ilmenite analyses were treated
 1190 by stoichiometric charge balance to calculate ferric relative to ferrous iron, thus generating the
 1191 ferric iron data used in the figure. Ilmenite compositions are subdivided following Wyatt et al.
 1192 (2004), with ilmenites considered to be indicators divided by the heavy, dashed orange line.
 1193 Among indicators, the extent of likely diamond preservation, based on modelled kimberlite
 1194 oxidation state (Gurney and Zweistra, 1995), is shown by the labelled fields separated by
 1195 heavy black lines. Canadian data from northern Baffin island and elsewhere in the NWT and
 1196 Nunavut derive from Northwest Territories Geological Survey, KIDD/KIMC (2017) and
 1197 Chidliak data derive from Pell and Nielson (2008)

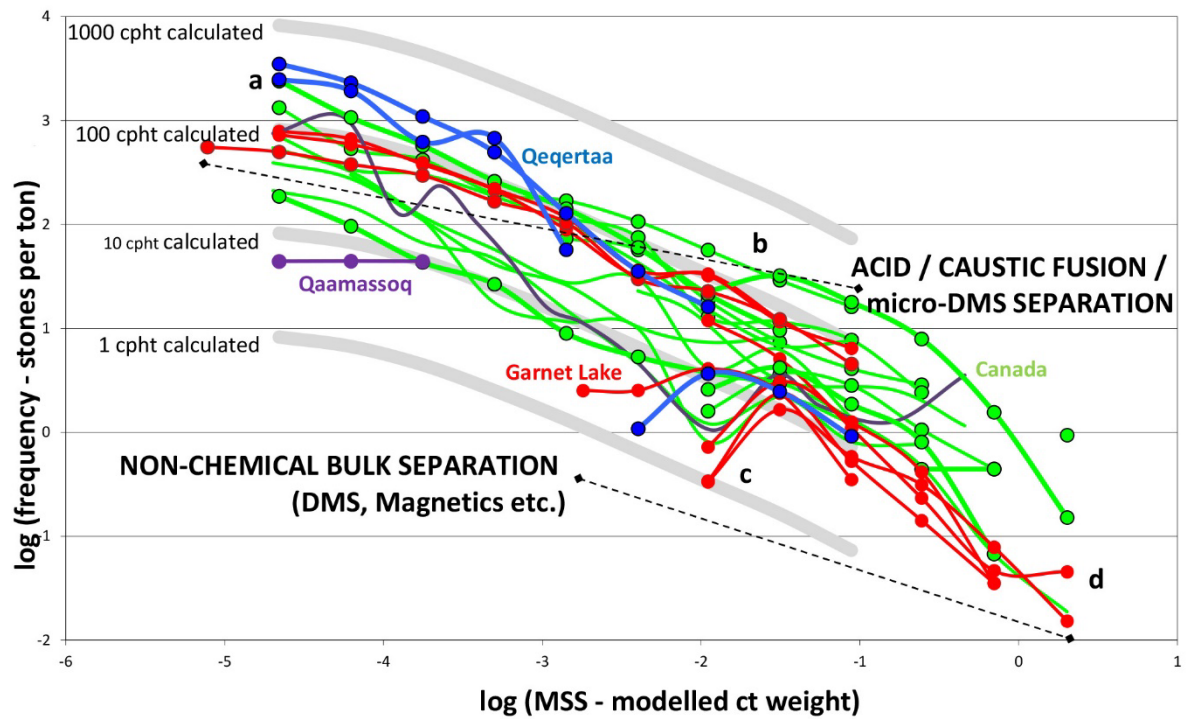


1198

1199

1200 **Fig. 11** Chemical composition of indicator spinels projected from the oxidized prism in terms
 1201 of Cr to Al ratio and Fe^{2+} to Mg ratio. Compositional fields coincident with chromite
 1202 inclusions in diamonds, kimberlite groundmass grains and xenocrysts in kimberlites have
 1203 been derived from Mitchell (1986). Projection onto the oxidized prism requires iron to be
 1204 calculated as ferrous and ferric. Greenland spinel compositions are presented following the
 1205 key. For comparison, the extent of 99% of Nunavut and Northwest Territories compositions
 1206 from Northwest Territories Geological Survey, KIDD/KIMC (2017) indicator spinels is
 1207 shown, as are individual compositions from the Brodeur Peninsula (Rae Craton in Canada)
 1208 from the same reference. Few chromites have compositions consistent with inclusions in
 1209 diamond. All of the Gardar Province, Ketilidian Orogen, NAC and Rae Craton show
 1210 compositions of spinel indicators consistent with both xenocrysts and phenocrysts in
 1211 kimberlites. The Rae Craton shows the widest compositional range. All Greenlandic regions
 1212 with spinel compositional data show strong similarity with data from diamond producing

1213 regions of Canada, including the rare, yet significant proportion of spinels with compositions
1214 in the diamond inclusion field



1215

1216

1217 **Fig. 12** Abundance of diamonds recovered according to size from Greenlandic and Canadian
 1218 exploration projects. Calculations of modelled stone size (MSS) following
 1219 methodology modified from Chapman and Boxer (2004). Garnet Lake data are shown
 1220 in red, Qeqertaa data are shown in blue and Qaamasoq data are shown in purple.
 1221 Canadian data are shown in green and derive from Stornoway Diamonds (Canada) Inc.
 1222 (2010 and 2011), Peregrine Diamonds Limited (2010 to 2012), Twin Mining
 1223 Corporation (2006), North Arrow Minerals Inc. (2015) and Diamondex Resources
 1224 Limited (2008) press releases and public technical reports, with industry-sourced data
 1225 references provided in Hutchison (2022). Data from the Chidliak kimberlites (later
 1226 acquired by De Beers) are indicated with green markers. Also, for comparison, the
 1227 data from a 1.5 tonne sample of the small, commercially mined kimberlite pipe at
 1228 Merlin (Lee et al., 1997) are shown with a solid black line. Diamonds recovered by
 1229 chemical means compared to non-chemical (DMS and magnetic) methods are
 1230 indicated by dashed lines. Qaamasoq recovery is not sufficiently large to fully assess
 1231 the diamond-potential of this locality

1232 **Tables**

1233

1234 **Table 1** Prospectivity scoring criteria based on sampling history (a), age of exposed rocks (b)
 1235 and mantle lithosphere characteristics (c)

(a) Sampling history scoring criteria

Ranking	Description	n	Ranking	Description	n
1	Reconnaissance-scale sampling (< 1 sample per 100 km ²) with good recovery (> 1/3 rd of samples are indicator positive)	2	4	Local-scale sampling with reasonable recovery or reconnaissance-scale with poor recovery (< 1/20 th of samples are indicator positive)	2
2	Regional-scale sampling (between 1 sample per 4 km ² and 1 sample per 100 km ²) with good recovery, or reconnaissance-scale with reasonable recovery (1/20 th to 1/3 rd of samples are indicator-positive)	5	5	Poor recovery from regional or local sampling density, or regions unsampled due to inaccessibility	7
3	Local-scale sampling (> 1 sample per 4 km ²) with good recovery or regional with reasonable recovery	2	6	No sampling conducted on geologically non-prospective regions	7

(b) Regional age range scoring criteria

1	All rocks are Archean and may, or may not predate the two recorded Archean carbonatites (2664 Ma Singertat Carbonatite Complex, Bizzarro et al., 2002; the 3007 Ma Tupertalik carbonatite, Blichert-Toft et al., 1995)	5	4	All rocks pre-date the Neoproterozoic diamond-prospective rocks, the oldest being the 603.6 Ma Tuttu lamprophyre (Secher et al., 2009), but they are younger than the Mesoproterozoic diamond-prospective rocks extending to the 1200 Ma Qassiarsuk Carbonatite (Andersen, 1997)	2
2	All rocks are Proterozoic and also pre-date the earliest Mesoproterozoic ultramafic lamprophyres (1299 Ma Grønnedal-Ika Complex, Secher et al., 2009), which include the diamondiferous Qeqertaa lamprophyre (possibly as old as 1962±80 Ma, Hutchison et al., 2024)	5	5	Some, or all rocks are older than the youngest diamond-prospective rock (Pyramidefjeld kimberlite, 149.8 Ma, Larsen et al., 2009), but all rocks are younger than than Neoproterozoic diamondiferous kimberlite / aillikite suite, which includes Garnet Lake and has its youngest manifestation with Goff's Dyke (555 Ma, Secher et al., 2009)	6
3	All rocks pre-date the Neoproterozoic diamond-prospective rocks (extending from the 603.6 Ma Tuttu lamprophyre, Secher et al., 2009), however, some overlap the Mesoproterozoic diamond-prospective rocks with the youngest age being 1200 Ma (Qassiarsuk Carbonatite, Andersen, 1997)	3	6	All rocks are younger than the youngest diamond-prospective rock (Pyramidefjeld kimberlite, 149.8 Ma, Larsen et al., 2009)	4

(c) Lithosphere thickness and density scoring criteria

1	Mean depth > 200km	2	4	Mean depth > 75 km and ≤ 125 km	5
2	Mean depth > 190 and ≤ 200 km	8	5	Mean depth < 75 km	4
3	Mean depth > 125 and ≤ 190 km	6			

1236

1237 n, number of regions assigned to each ranking

1238

Table 2 Prospectivity scores and rankings of Greenlandic geological regions

Region	Sampling score	Age score	Lithosphere score	Cumulative score	Prospectivity
Caledonian Orogen basement	5*	2	4	11	8
Caledonian Orogen intrusives	6	5	5	16	12
Cenozoic Basins	6	6	3	15	11
Devonian Basin of East Greenland	6	5	5	16	12
East Greenland Rift Basin	6	5	5	16	12
Eleanore Bay Basin	5*	4	4	13	9
Franklinian Basin	1	5	3	9	6
Gardar Province	2	3	2	7	4
Hagen Fjord - Hekla Sund Basin	5*	4	4	13	9
Iapetus Ocean Margin	6	5	5	16	12
Independence Fjord Basin	5*	3	3	11	8
Inglefield Orogenic Belt	1	2	2	5	2
Kangerlussuaq Basin	6	6	3	15	11
Karrat Basin	3	2	2	7	4
Ketilidian Orogen	2	2	2	6	3
NAC (eastern Greenland)	2	1	3	6	3
NAC (western Greenland)	2	1	1	4	1
NAIP	4	6	4	14	10
Nuussuaq Basin	3	6	2	11	8
Prøven Igneous Complex	5	2	2	9	6
Rae Craton (eastern Greenland)	4	1	3	8	5
Rae Craton (north Greenland)	5*	1	2	8	5
Rae Craton (western Greenland)	2	1	1	4	1
Thule Basin	5*	3	2	10	7

Region	Sampling score	Age score	Lithosphere score	Cumulative score	Prospectivity
Wandel Sea Basin	6	5	4	15	11

1240

1241 NAIP = North Atlantic Igneous Province

1242 * Sampling score modified from 6 to 5 because region was not neglected due to low perceived
 1243 prospectivity, rather due to logistical factors

Supplementary Table 1 Sampling metrics and scoring by geological region

Region	Area (km ²)	Total onshore samples	DIM and diamond processed samples	Samples per 100 x 100 km area	% of indicator-positive samples	Initial score	Adjusted score*
Caledonian Orogen basement	35 663	1024	0	0	na	6	5
Caledonian Orogen intrusives	4996	789	0	0	na	6	6
Cenozoic Basins	312	3	0	0	na	6	6
Devonian Basin of E Greenland	8805	218	0	0	na	6	6
E Greenland Rift Basin	16 150	2077	0	0	na	6	6
Eleanore Bay Basin	24 601	2271	0	0	na	6	5
Franklinian Basin	74 110	57	57	7.7	82	1	1
Gardar Province	1147	12	12	104.6	42	2	2
Hagen Fjord - Hekla Sund Basin	8183	0	0	0	na	6	5
Iapetus Ocean Margin	809	68	0	0	na	6	6
Independence Fjord Basin	19 168	0	0	0	na	6	5
Inglefield Orogenic Belt	5377	1	1	1.9	100	1	1
Kangerlussuaq Basin	809	0	0	0	na	6	6
Karrat Basin	7150	105	93	130.1	6	3	3
Ketilidian Orogen	17 646	471	467	264.6	52	2	2
NAC (eastern Greenland)	10 471	780	232	221.6	50	2	2
NAC (western Greenland)	45 231	11 288	10 367	2292.0	67	2	2
NAIP	24 931	213	3	1.2	0	4	4
Nuussuaq Basin	17 515	242	242	138.2	17	3	3
Prøven Igneous Complex	2780	33	33	118.7	0	5	5

Region	Area (km ²)	Total onshore samples	DIM and diamond processed samples	Samples per 100 x 100 km area	% of indicator-positive samples	Initial score	Adjusted score*
Rae Craton (eastern Greenland)	20 829	423	10	4.8	0	4	4
Rae Craton (north Greenland)	276	0	0	0	na	6	5
Rae Craton (western Greenland)	45 771	4921	4436	969.2	77	2	2
Thule Basin	5329	0	0	0	na	6	5
Wandel Sea Basin	3456	0	0	0	na	6	6

1245

1246 NAIP = North Atlantic Igneous Province, na = not applicable

1247 * Regions with no sampling initially score 6, by definition. However, where sampling has

1248 been absent due to non-geological reasons (such as inaccessibility), such regions are assigned

1249 a score of 5, matching those with poor recovery despite sampling being conducted at local or

1250 regional-scale